ISSI, 26/02/2018

Quasi-Periodic Pulsation in a microflare on 25/01/2017

Nakariakov, V.M.

University of Warwick, UK

S. Anfinogentov, V.M. Bogod, E. A. Kurochkin, I. N. Sharykin, T. I. Kaltman

One should be careful with wavelets:

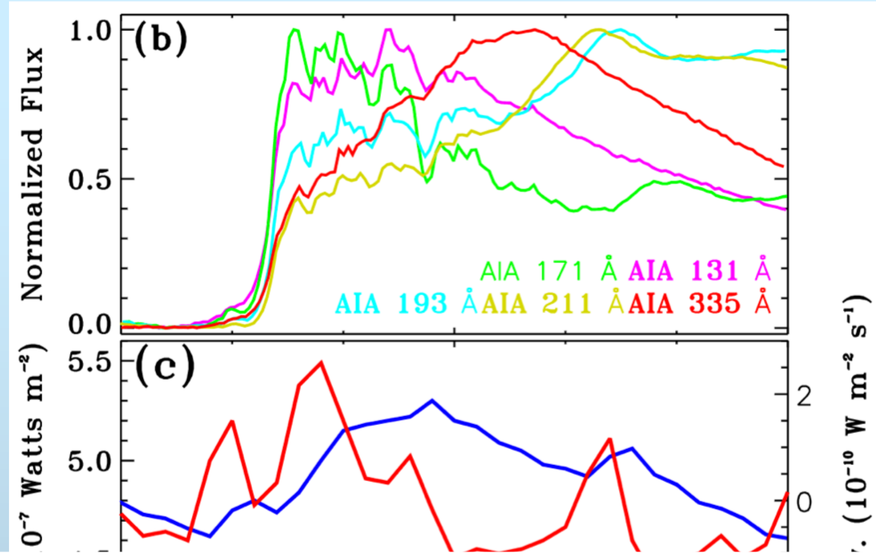

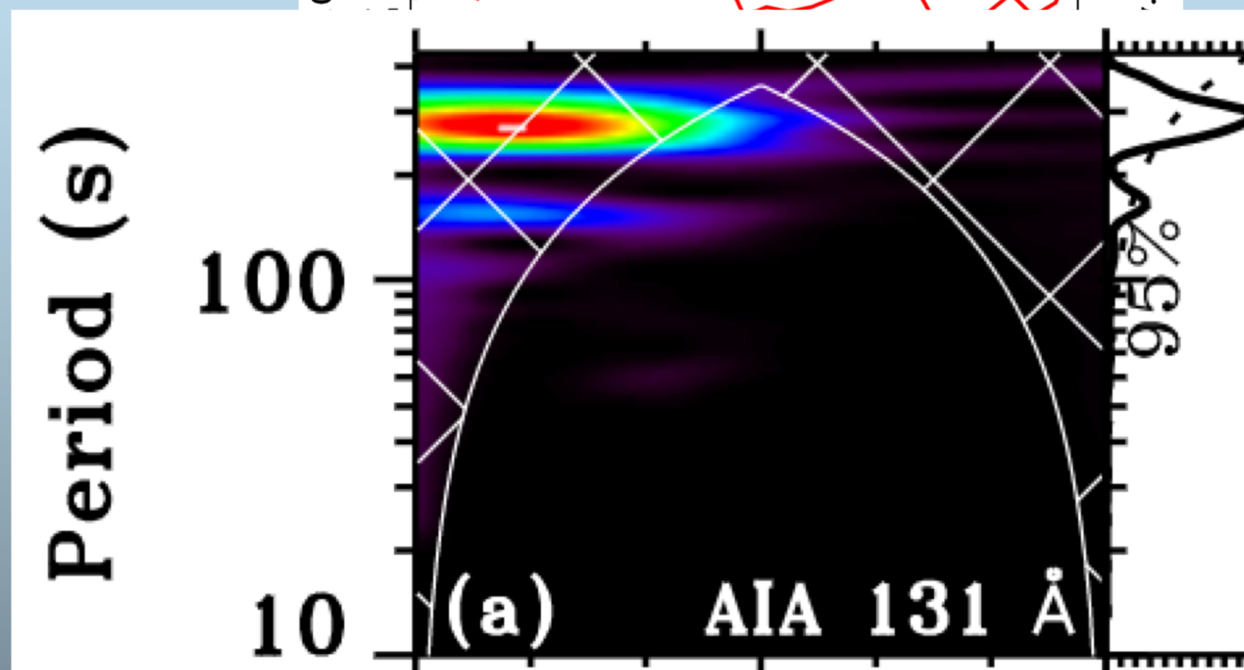

What do we mean by QPP in a flare?

c.f. Pc and Pi in the Earth's magnetosphere

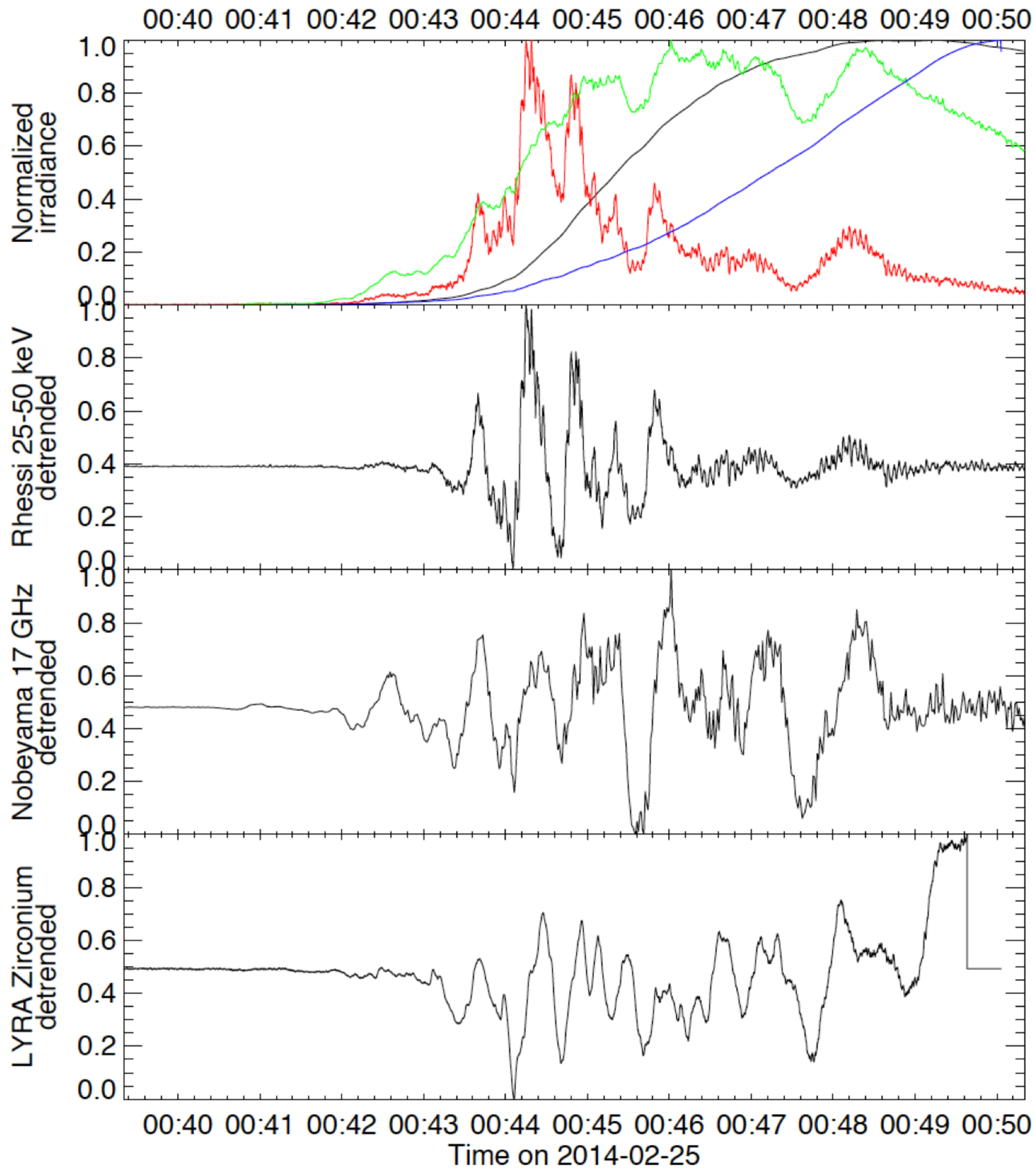

WARWICK

Space Sci Rev (2018) 214:45
https://doi.org/10.1007/s11214-018-0478-5

Contents

Modelli
Flares

J.A. McLa
M. Domini

Received: 19 I

Abstract S
of solar ene
shows a pro
of a second
tions (QPPs), to emphasise that they often contain apparent amplitude and period modulation. We review the current understanding of quasi-periodic pulsations in solar and stellar flares. In particular, we focus on the possible physical mechanisms, with an emphasis

hysics

Mechanisms for QPP:

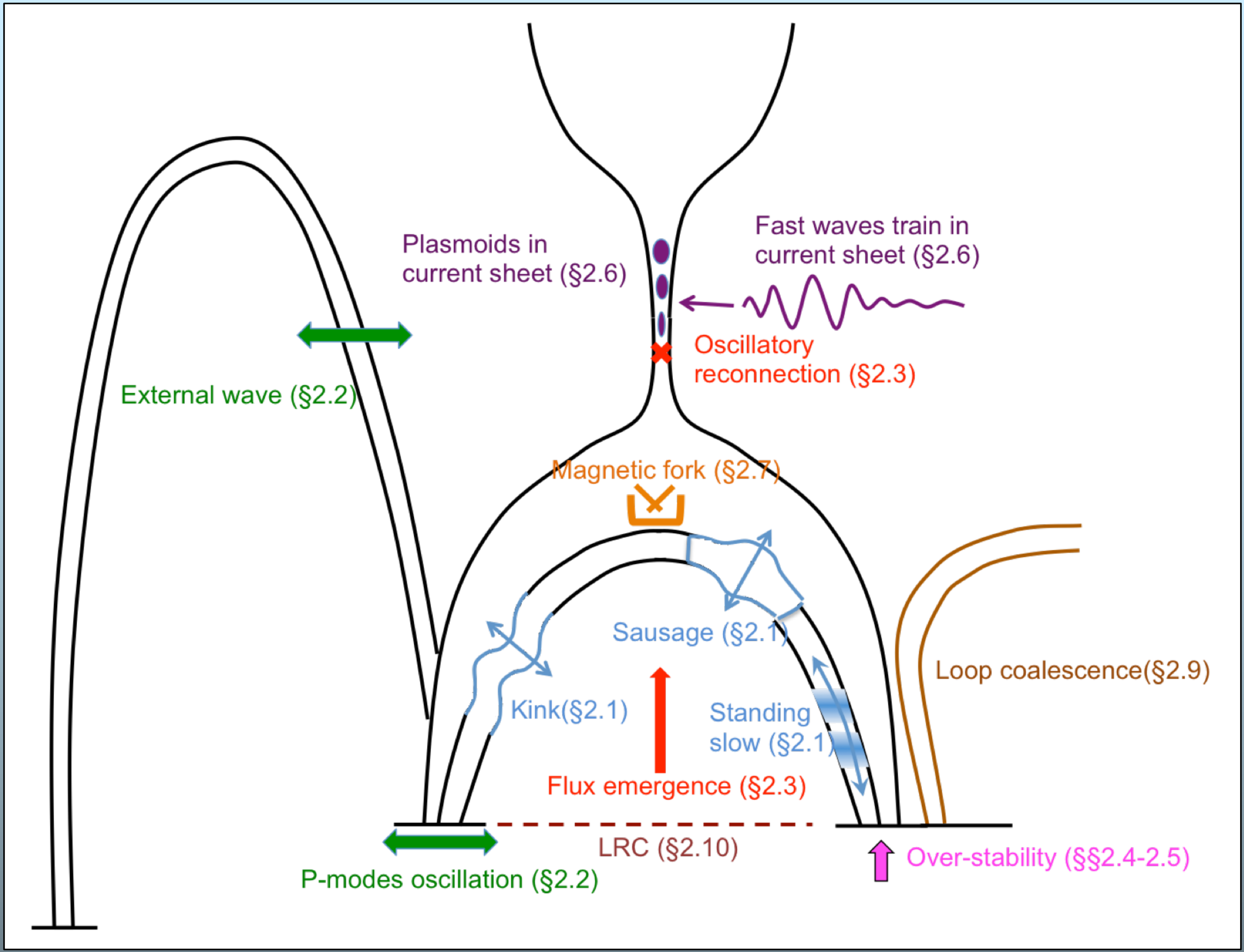

QPP in microflares:

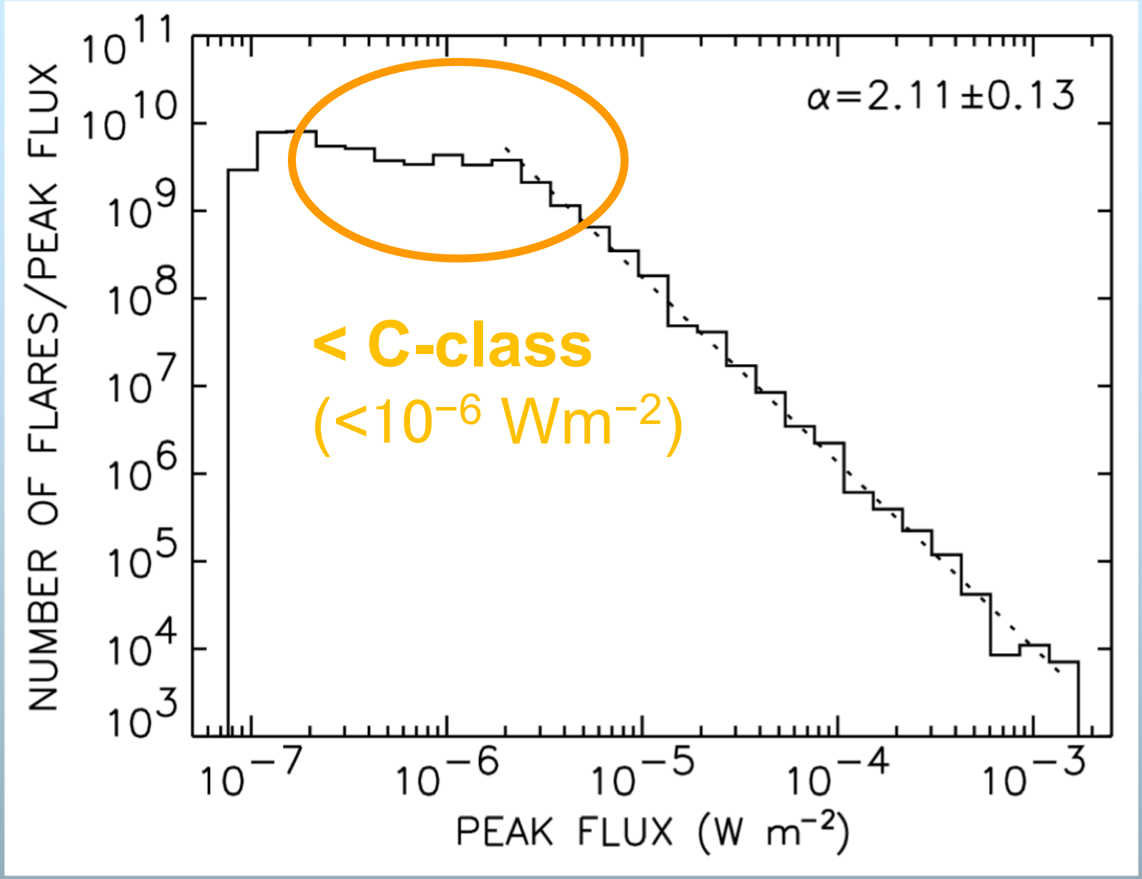

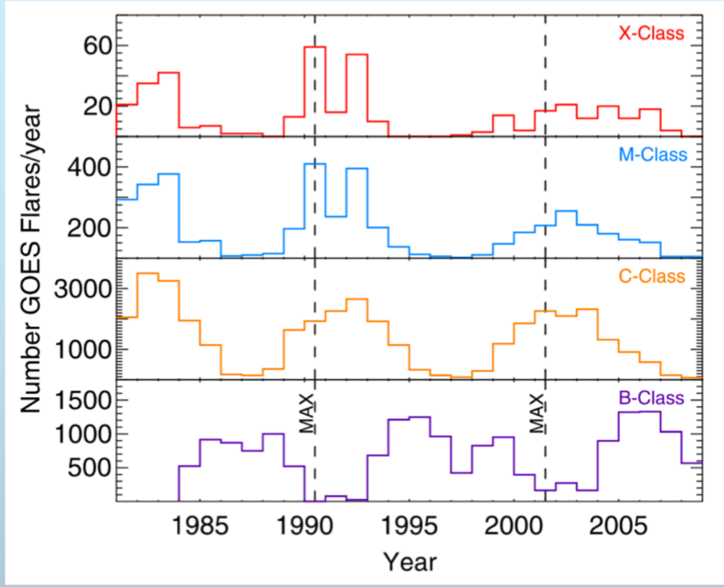

- Are physical mechanisms in microflares the same as in more powerful flares?
- Are properties of QPP in microflares the same as in more powerful flares?

Radio Astronomical Telescope of the Academy of Sciences - 600

ATAN-600 parameters for solar observations:

4 -constructed:

flector-type transit radio telescope, ring with ~ 600 m diameter;

ollecting area 1,200 m^2;

) imaging due to Earth rotation with FWHM ~ 9’’x7.5’ x λ;

pectral range 1-30 GHz, 6 discrete wavelengths

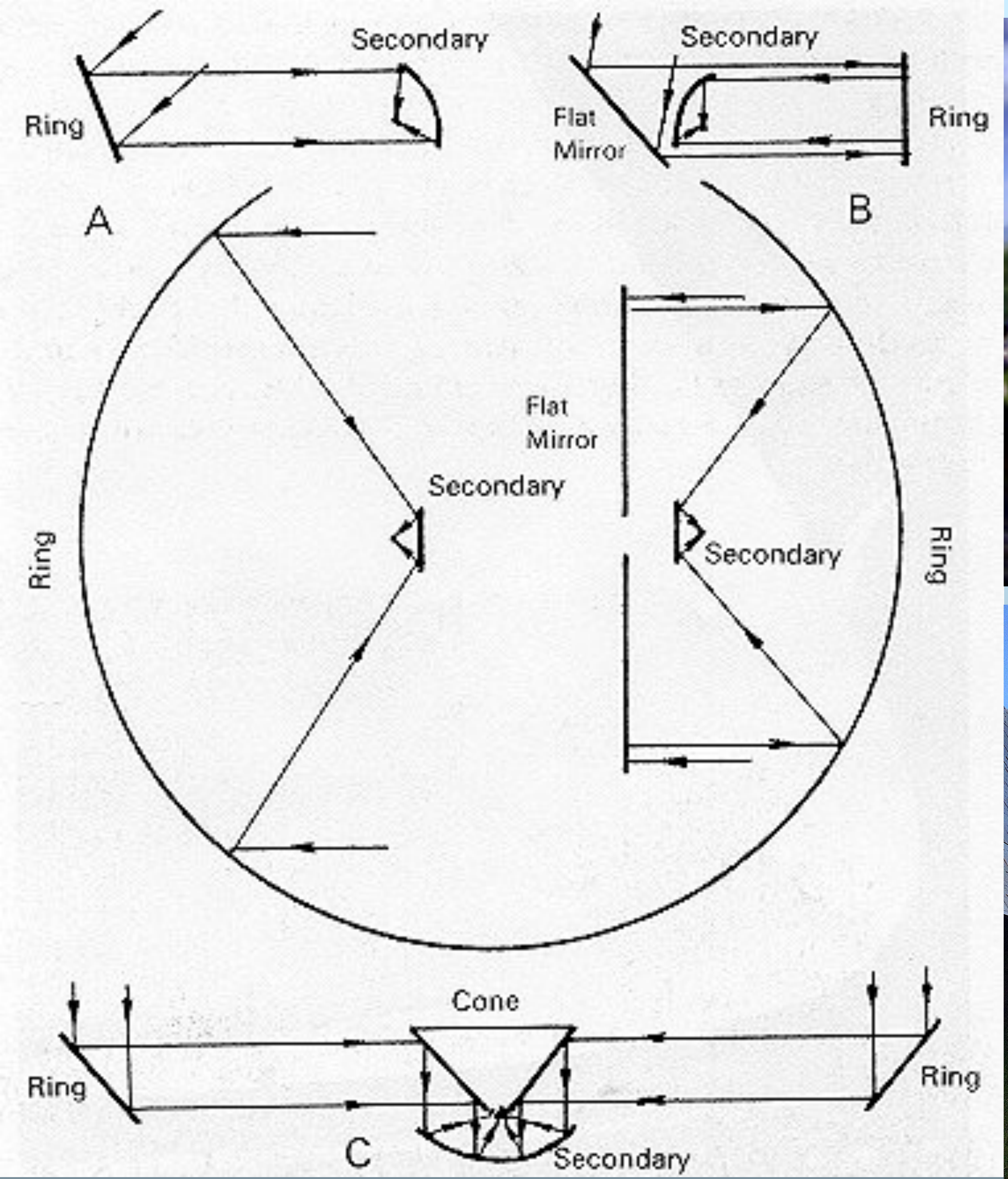
Secondary
Ring
A
Secondary
Flat
Mirror
Ring
B
Ring
Flat
Mirror
Secondary
Secondary
Ring
Cone
Ring
Ring
C
Secondary

RATAN-600 is able to detect microflares,
but it requires the flaring AR passing through the observational slit exactly when the flare occurs.

Hence, usually long-durational, e.g.:

198 BOGOD

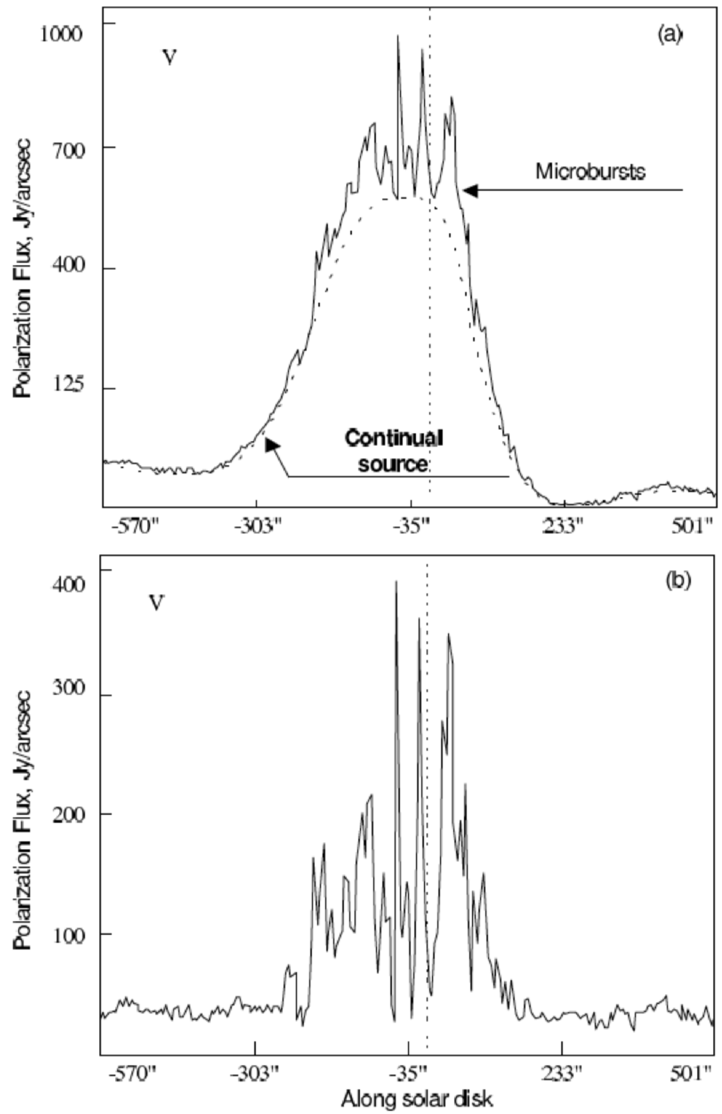

Fig. 3. Decimeter-wave emission in the active region at 31.41 cm. The upper panel shows a scan of the active region, where the burst and continuum components can be seen. The lower panel shows the extracted microburst component [51].

Microflare on 25/01/2017

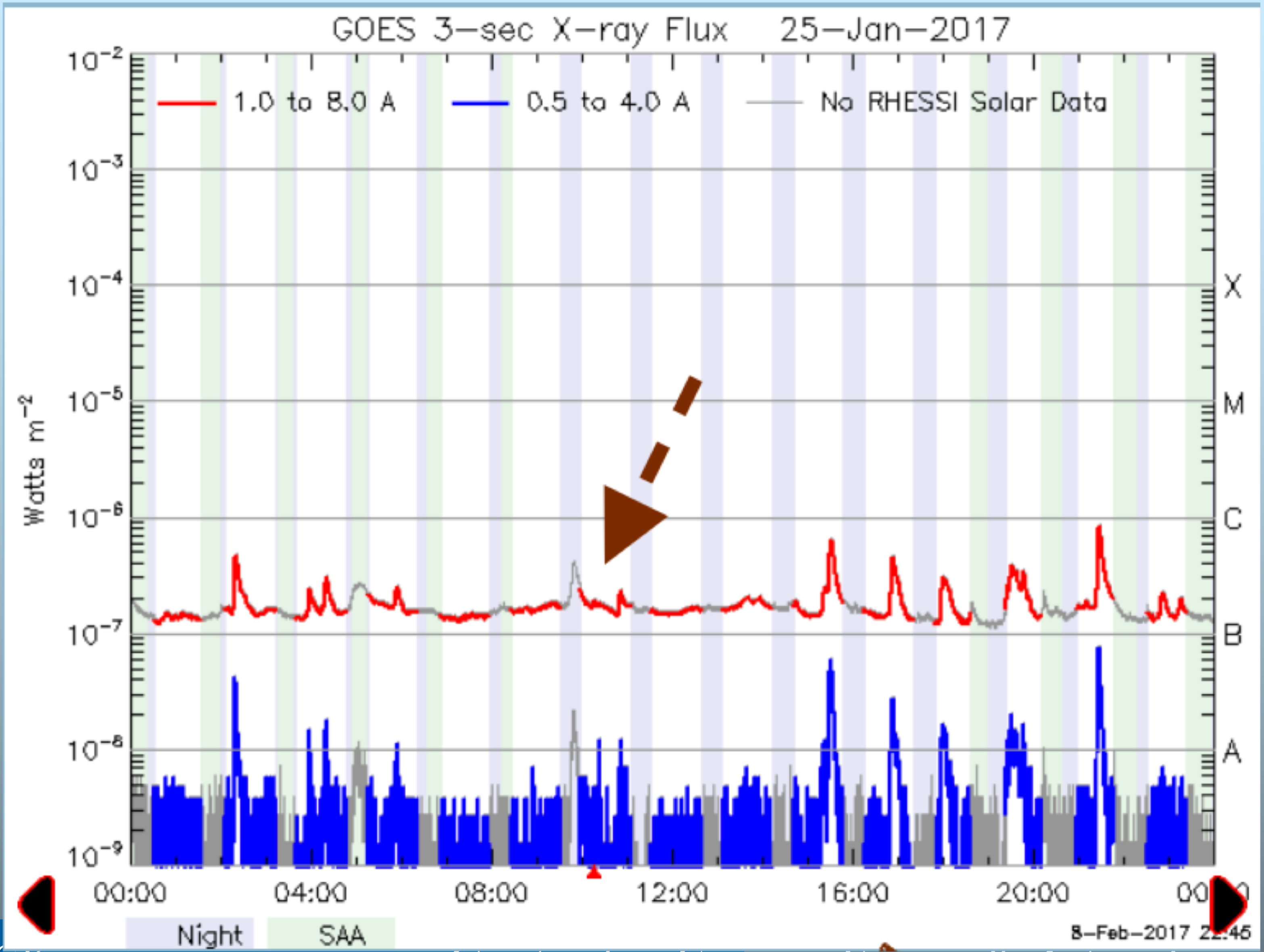

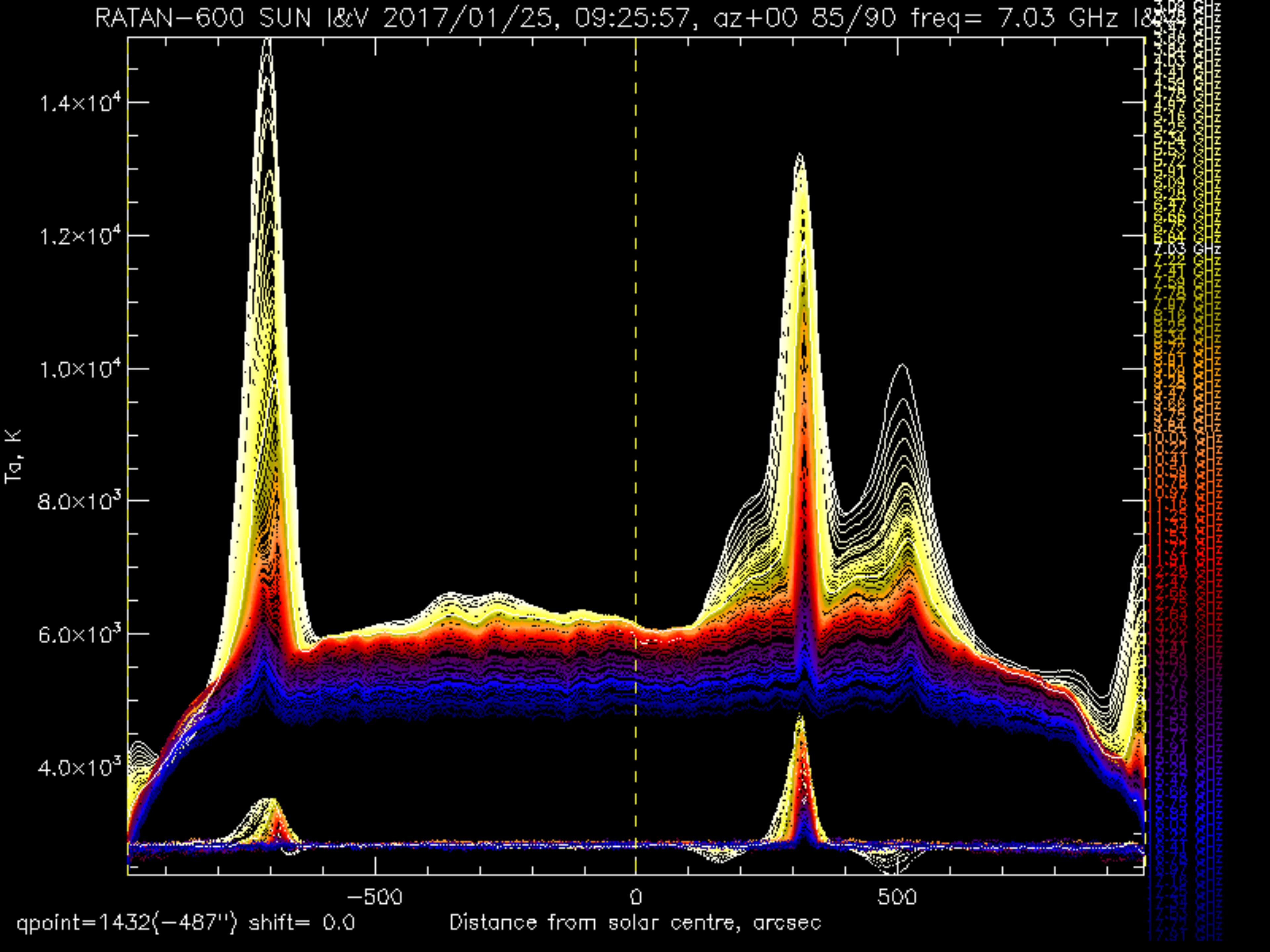
RATAN-600 SUN I&V 2017/01/25, 09:25:57, az+00 85/90 freq= 7.03 GHz
Ta, K
1.4×10^4
1.2×10^4
1.0×10^4
8.0×10^3
6.0×10^3
4.0×10^3
−500
0
500
Distance from solar centre, arcsec
qpoint=1432(−487") shift= 0.0
7.03 GHz

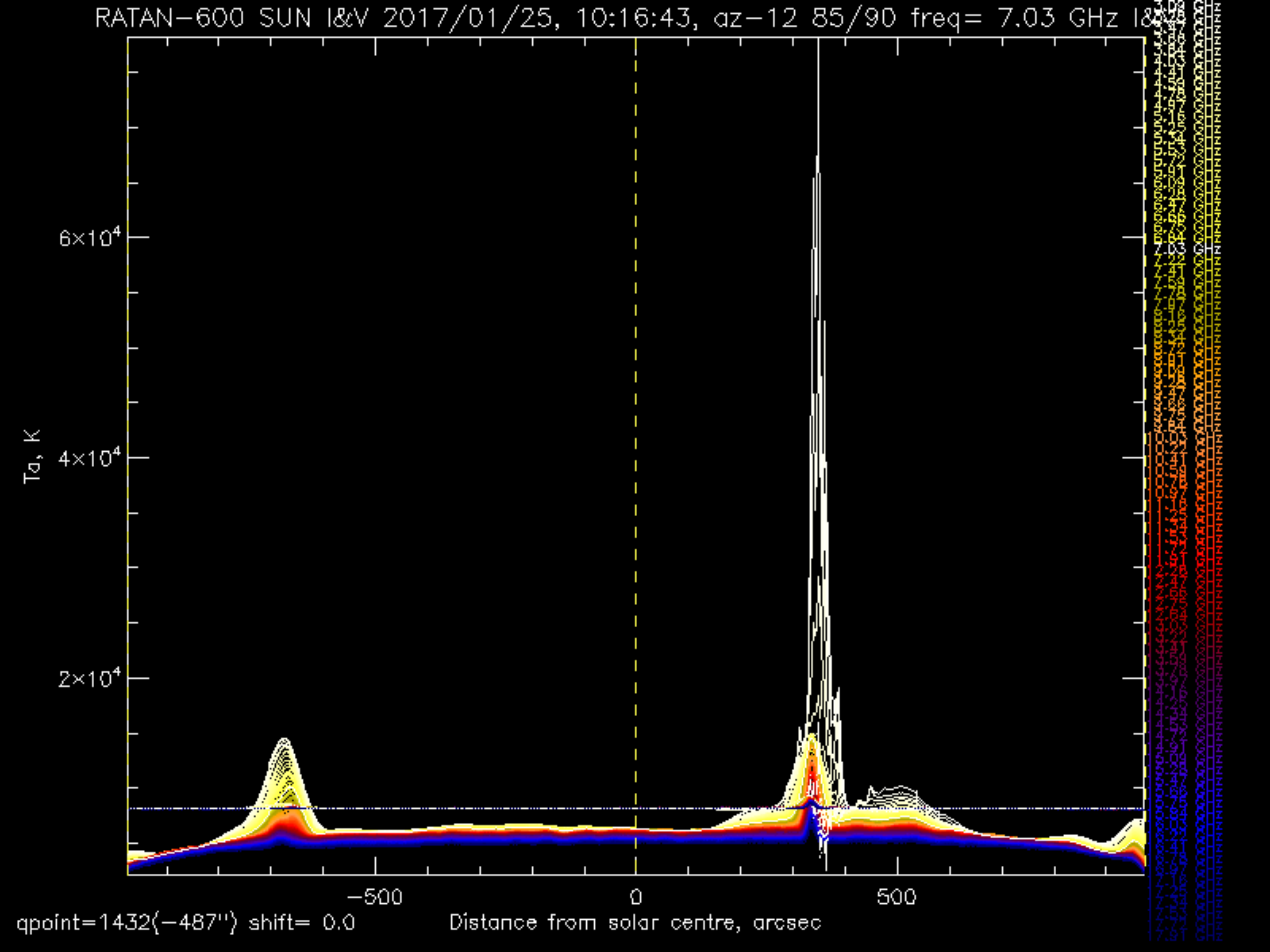

RATAN-600 SUN I&V 2017/01/25, 10:16:43, az-12 85/90 freq= 7.03 GHz I&
Ta, K
6×10^4
4×10^4
2×10^4
-500
0
500
7.03 GHz
qpoint=1432(-487") shift= 0.0
Distance from solar centre, arcsec

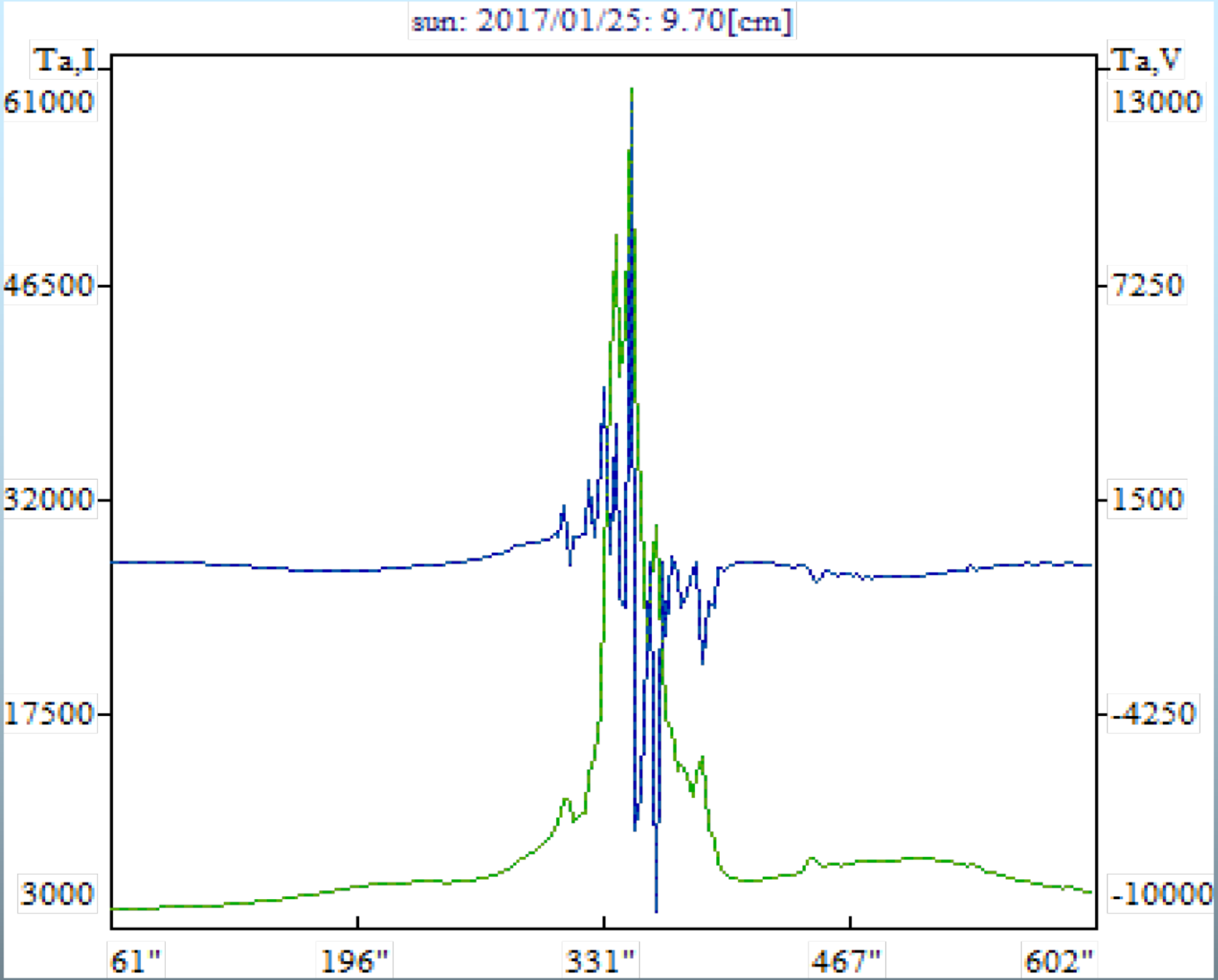
sun: 2017/01/25: 9.70[cm]
Ta,I
61000
46500
32000
17500
3000
Ta,V
13000
7250
1500
-4250
-10000
61"
196"
331"
467"
602"

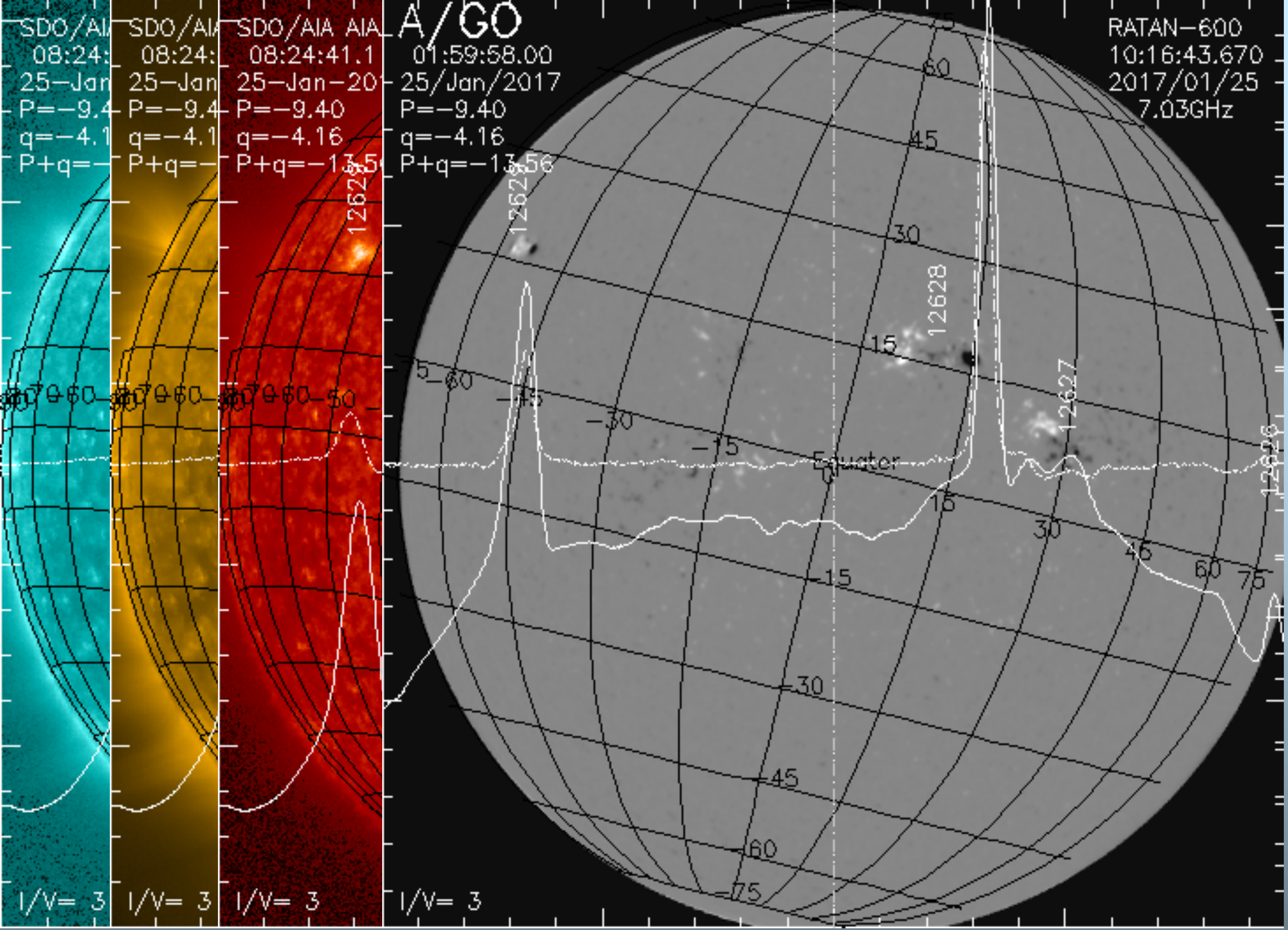

SDO/AIA
08:24:41.1
25-Jan-20
P=-9.40
q=-4.16
P+q=-13.56
A/GO
01:59:58.00
25/Jan/2017
RATAN-600
10:16:43.670
2017/01/25
7.03GHz
12628
12627
12626
Equator
I/V= 3

The central meridian corresponds to the 1604th count, the **maximum emission** to the 1726th count, thus the maximum emission is detected at **10:16:18 UT** (= 10:16:43 UT - 122x0.2s)

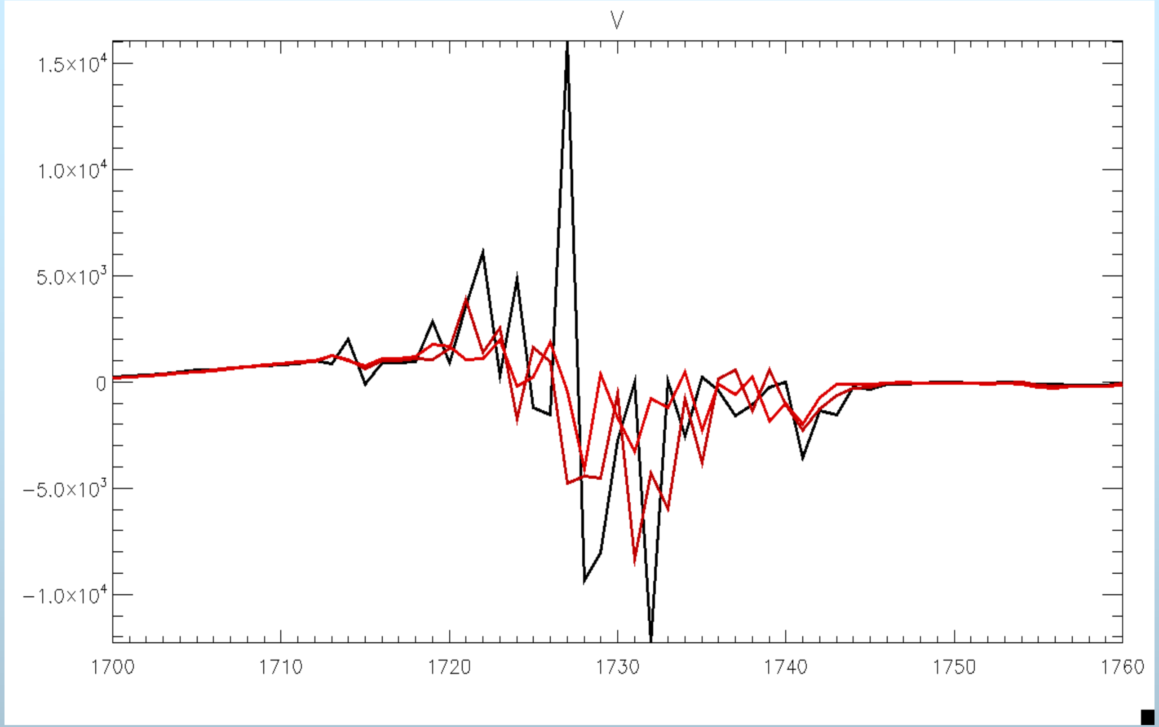

The event lasts from count 1713 to count 1744. As the central meridian is in count 1604 at 10:16:43, we get the time of the event **from about 10:16:15 to 10:16:21**.

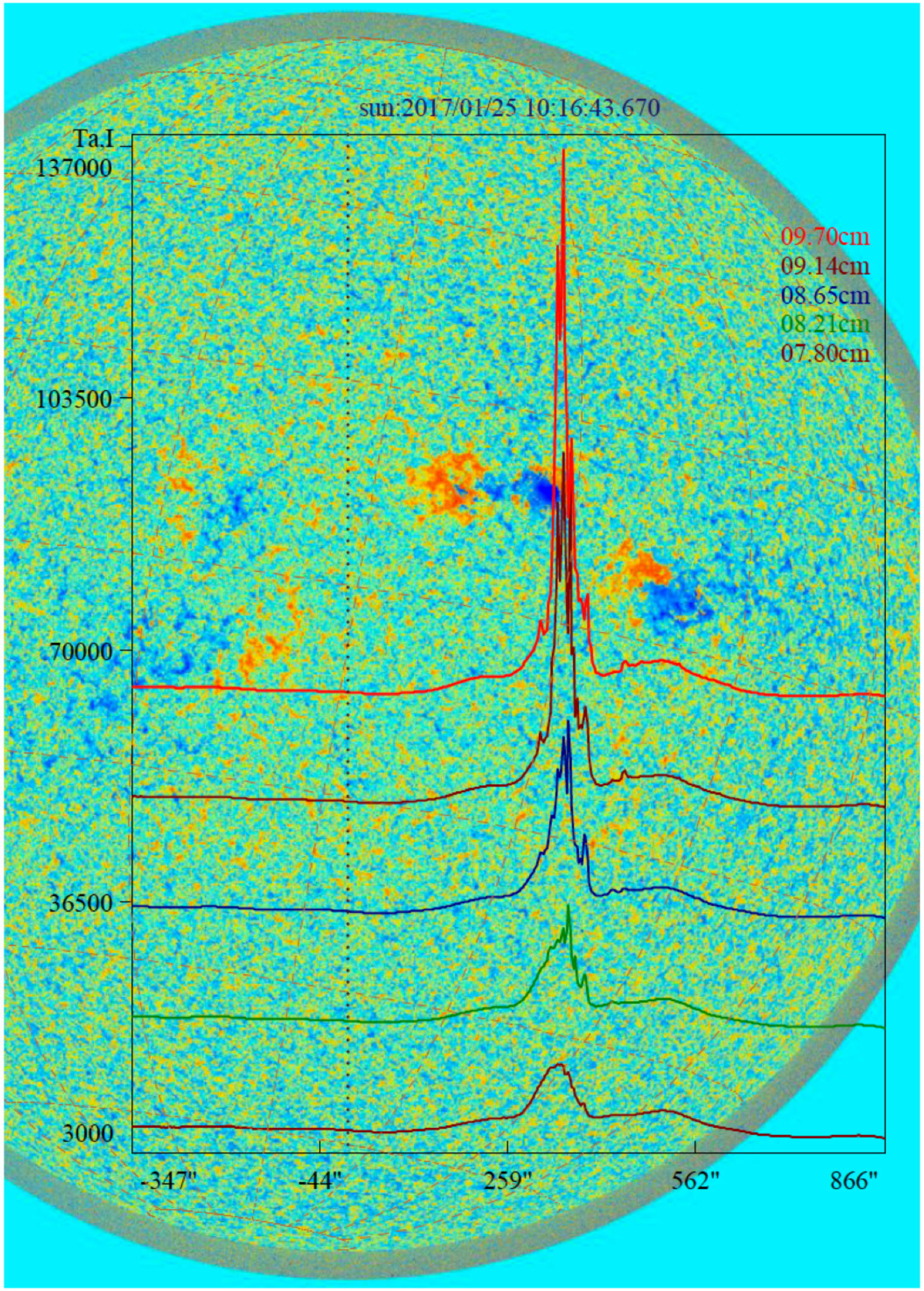
sun:2017/01/25 10:16:43.670
Ta.I
137000
103500
70000
36500
3000
-347''
-44''
259''
562''
866''
09.70cm
09.14cm
08.65cm
08.21cm
07.80cm

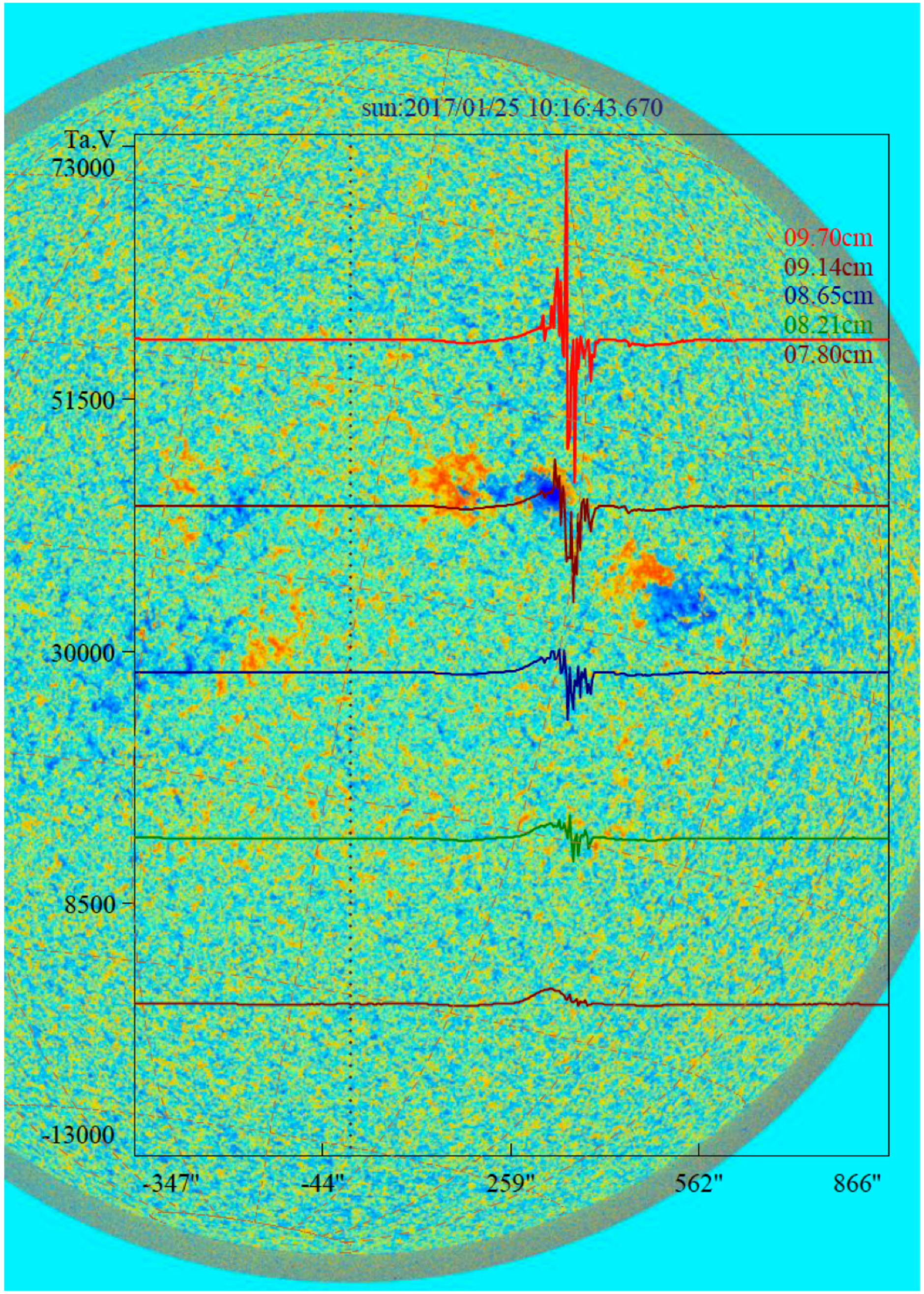
sun:2017/01/25 10:16:43.670
Ta.V
73000
51500
30000
8500
-13000
-347''
-44''
259''
562''
866''
09.70cm
09.14cm
08.65cm
08.21cm
07.80cm

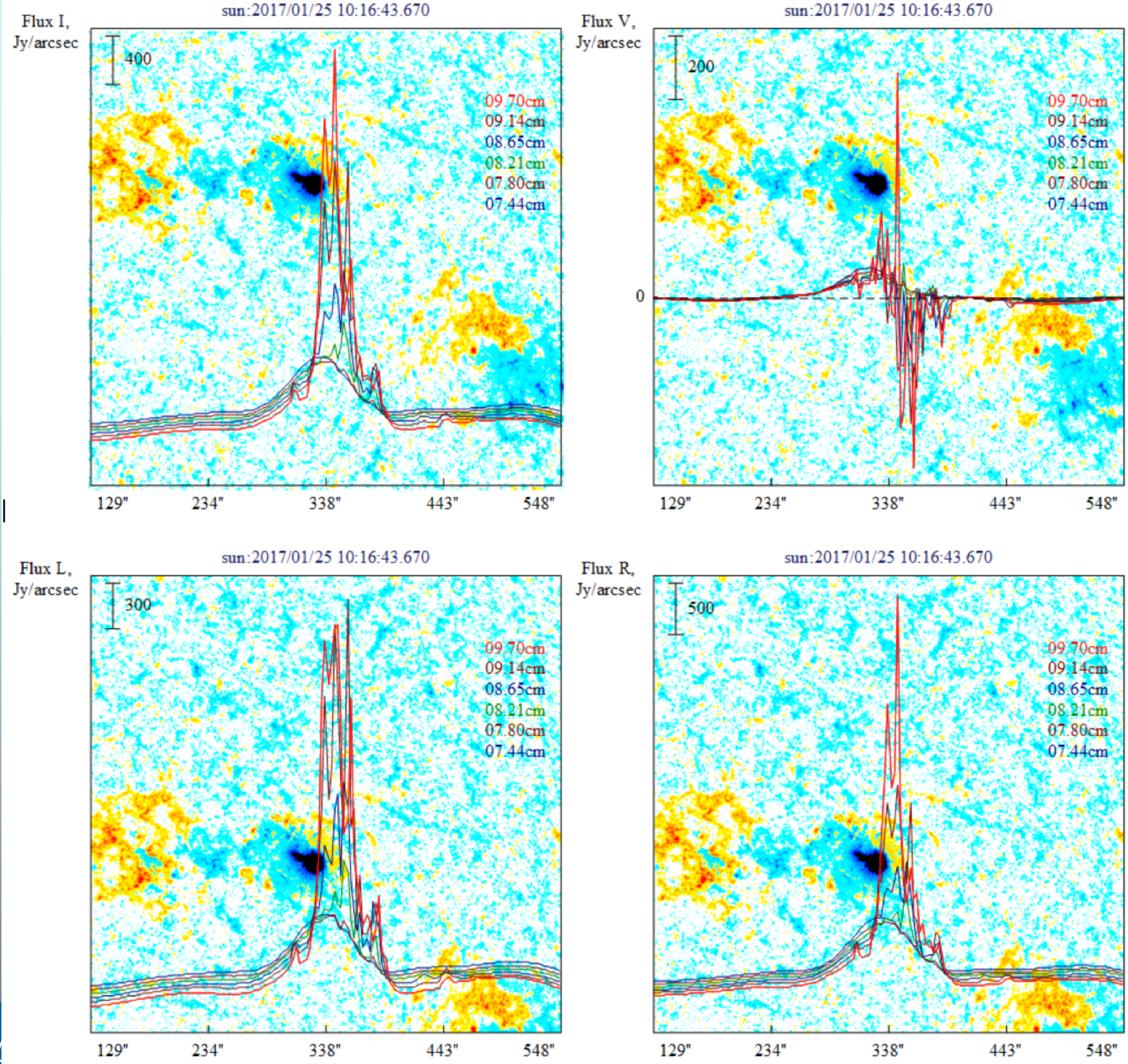

Flux I, Jy/arcsec
sun:2017/01/25 10:16:43.670
400
09.70cm
09.14cm
08.65cm
08.21cm
07.80cm
07.44cm
129"
234"
338"
443"
548"
Flux V, Jy/arcsec
sun:2017/01/25 10:16:43.670
200
0
09.70cm
09.14cm
08.65cm
08.21cm
07.80cm
07.44cm
129"
234"
338"
443"
548"
Flux L, Jy/arcsec
sun:2017/01/25 10:16:43.670
300
09.70cm
09.14cm
08.65cm
08.21cm
07.80cm
07.44cm
129"
234"
338"
443"
548"
Flux R, Jy/arcsec
sun:2017/01/25 10:16:43.670
500
09.70cm
09.14cm
08.65cm
08.21cm
07.80cm
07.44cm
129"
234"
338"
443"
548"

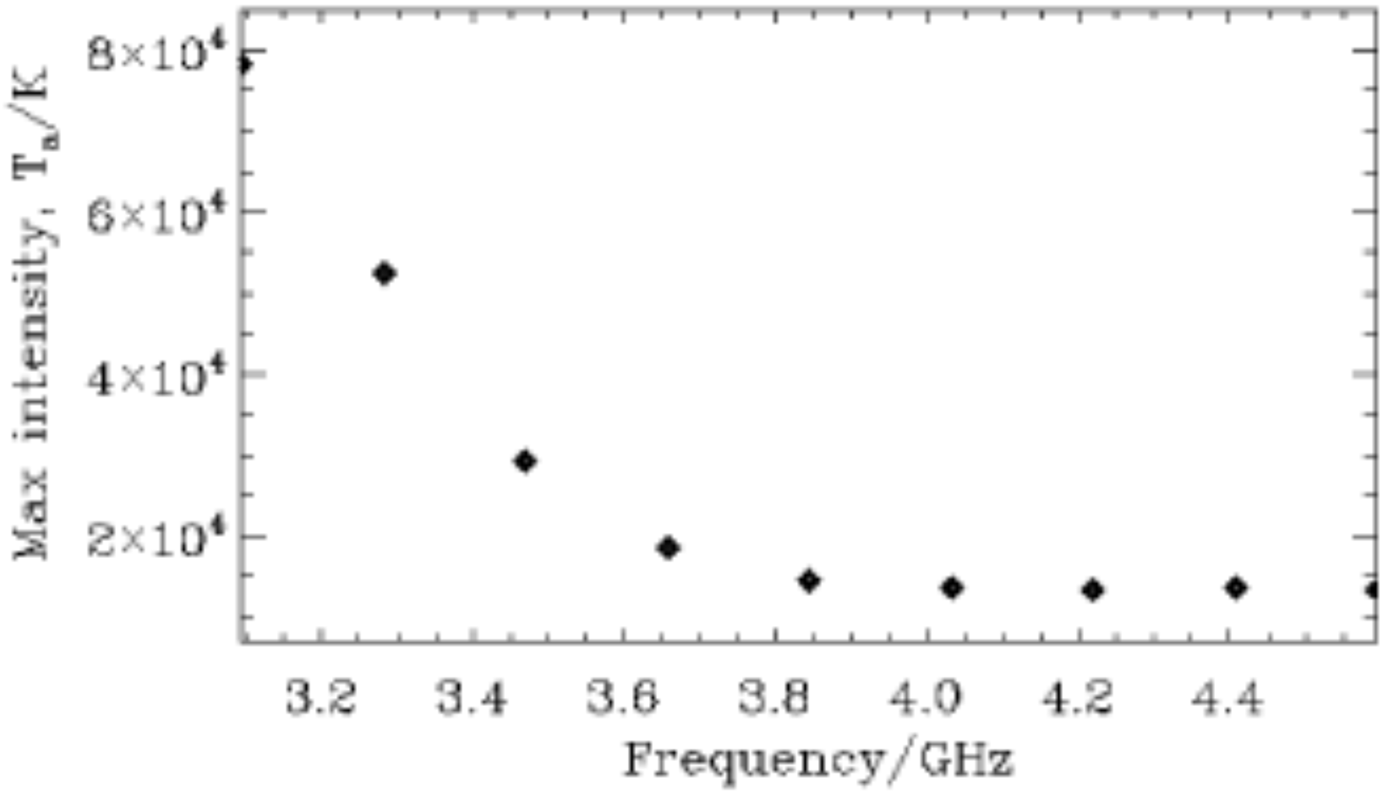

Fig. 5.— Dependence of the radio burst intensity on the frequency at 10:16:20 UT.

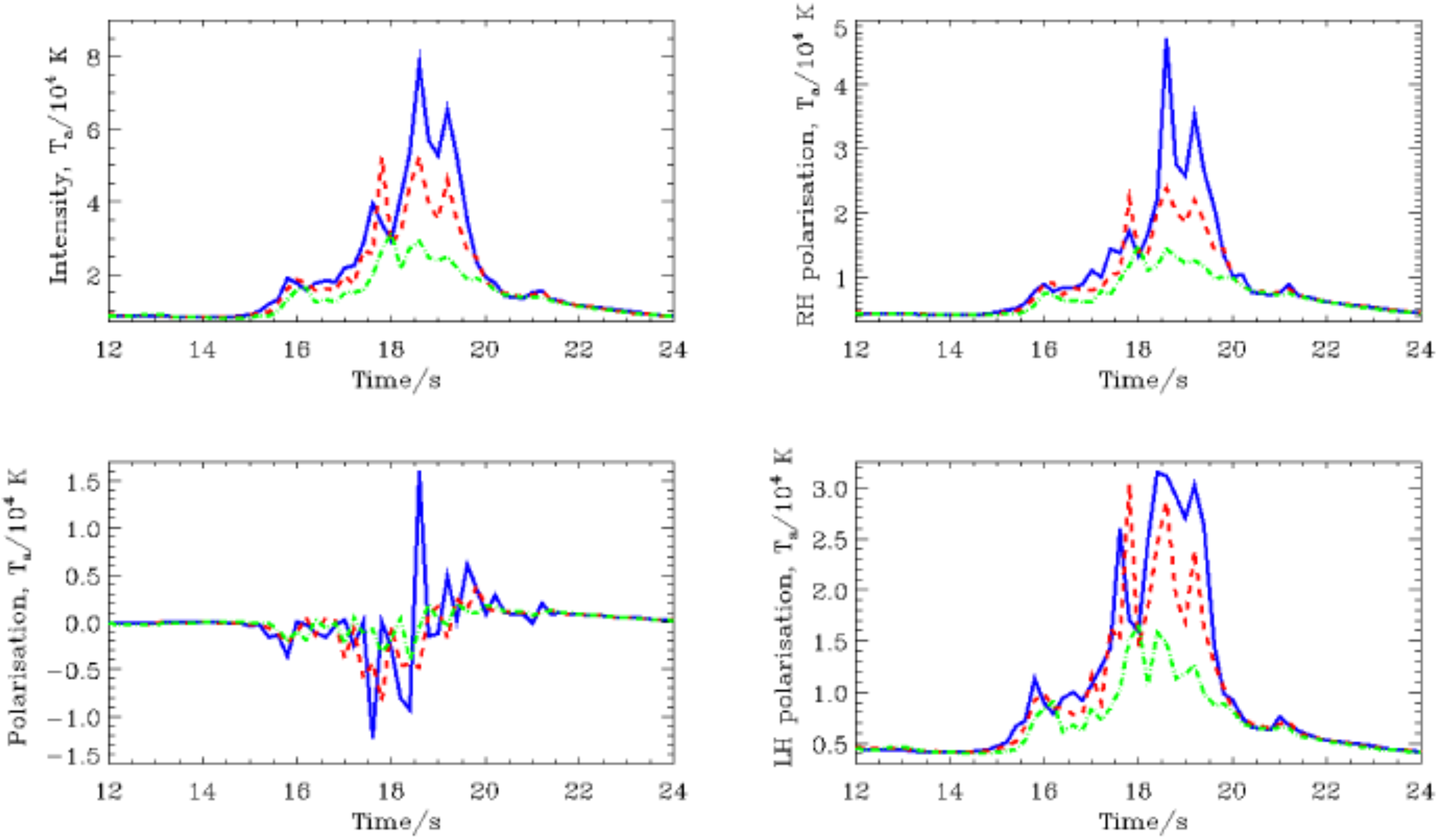
Intensity, $T_a/10^4$ K
RH polarisation, $T_a/10^4$ K
Polarisation, $T_a/10^4$ K
LH polarisation, $T_a/10^4$ K
Time/s
Time/s
Time/s
Time/s
12 14 16 18 20 22 24
2 4 6 8
1 2 3 4 5
−1.5 −1.0 −0.5 0.0 0.5 1.0 1.5
0.5 1.0 1.5 2.0 2.5 3.0

10:16:15 - 10:16:21 UT

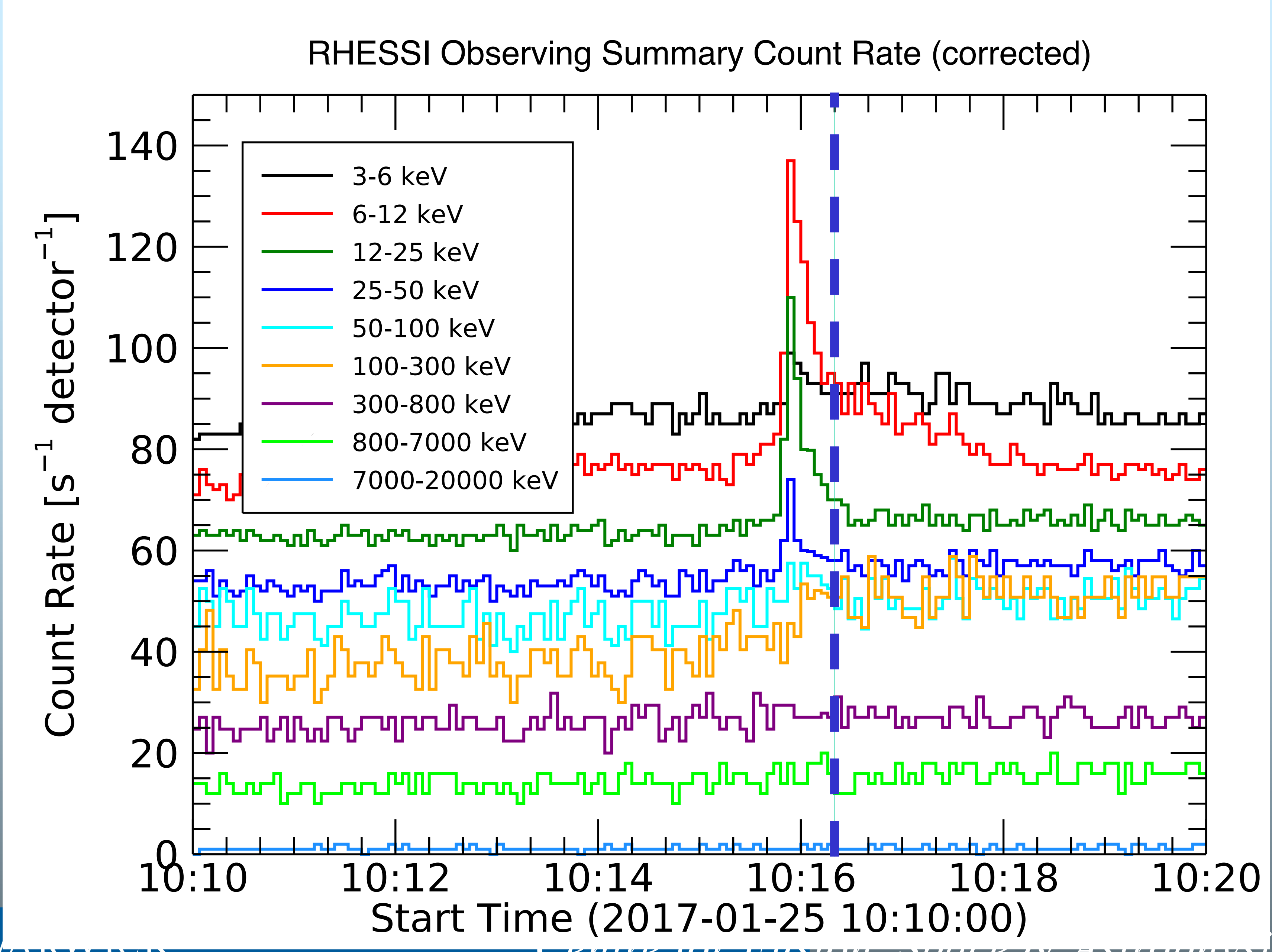

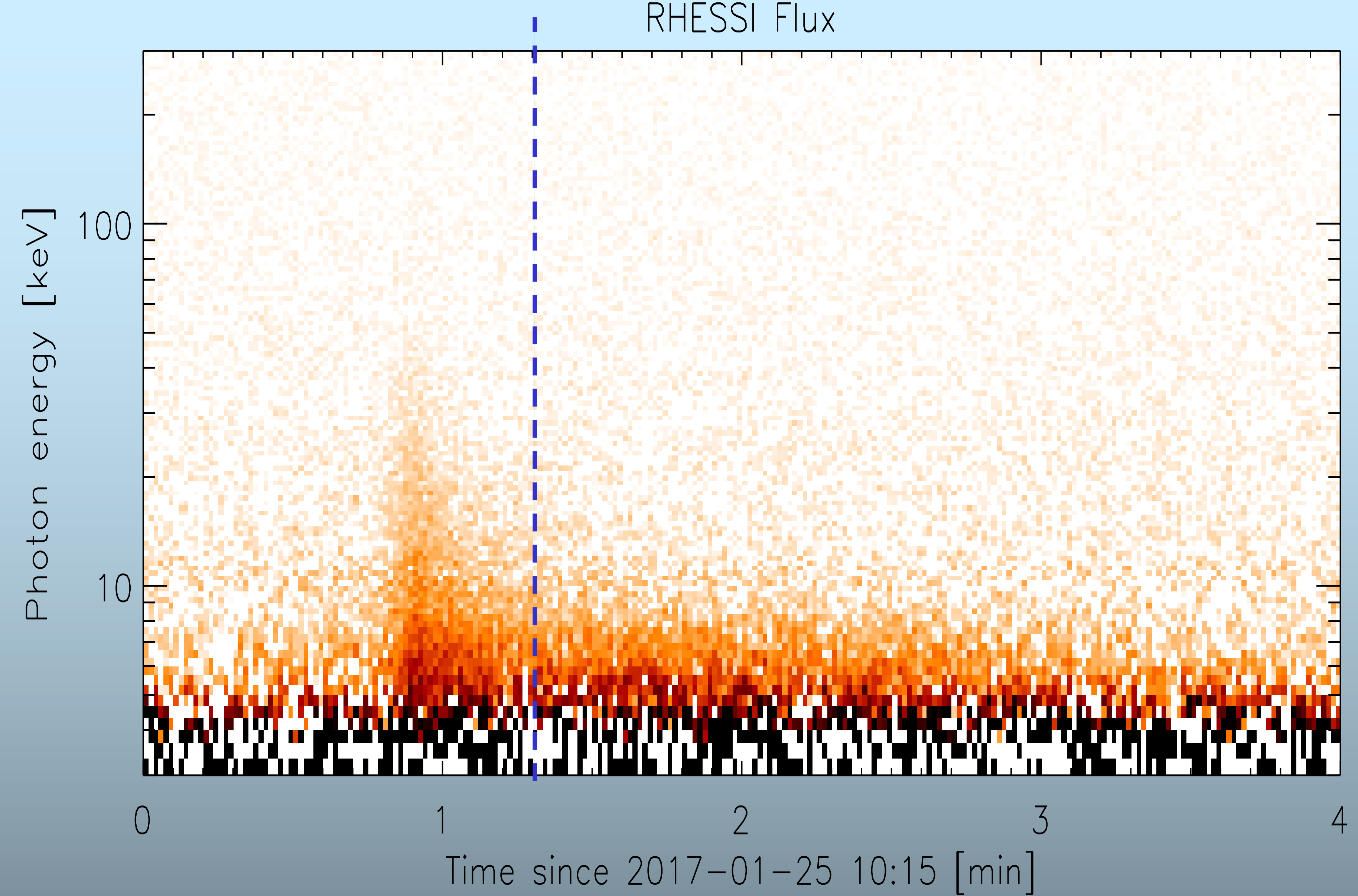

RHESSI Flux
Photon energy [keV]
100
10
0
1
2
3
4
Time since 2017-01-25 10:15 [min]

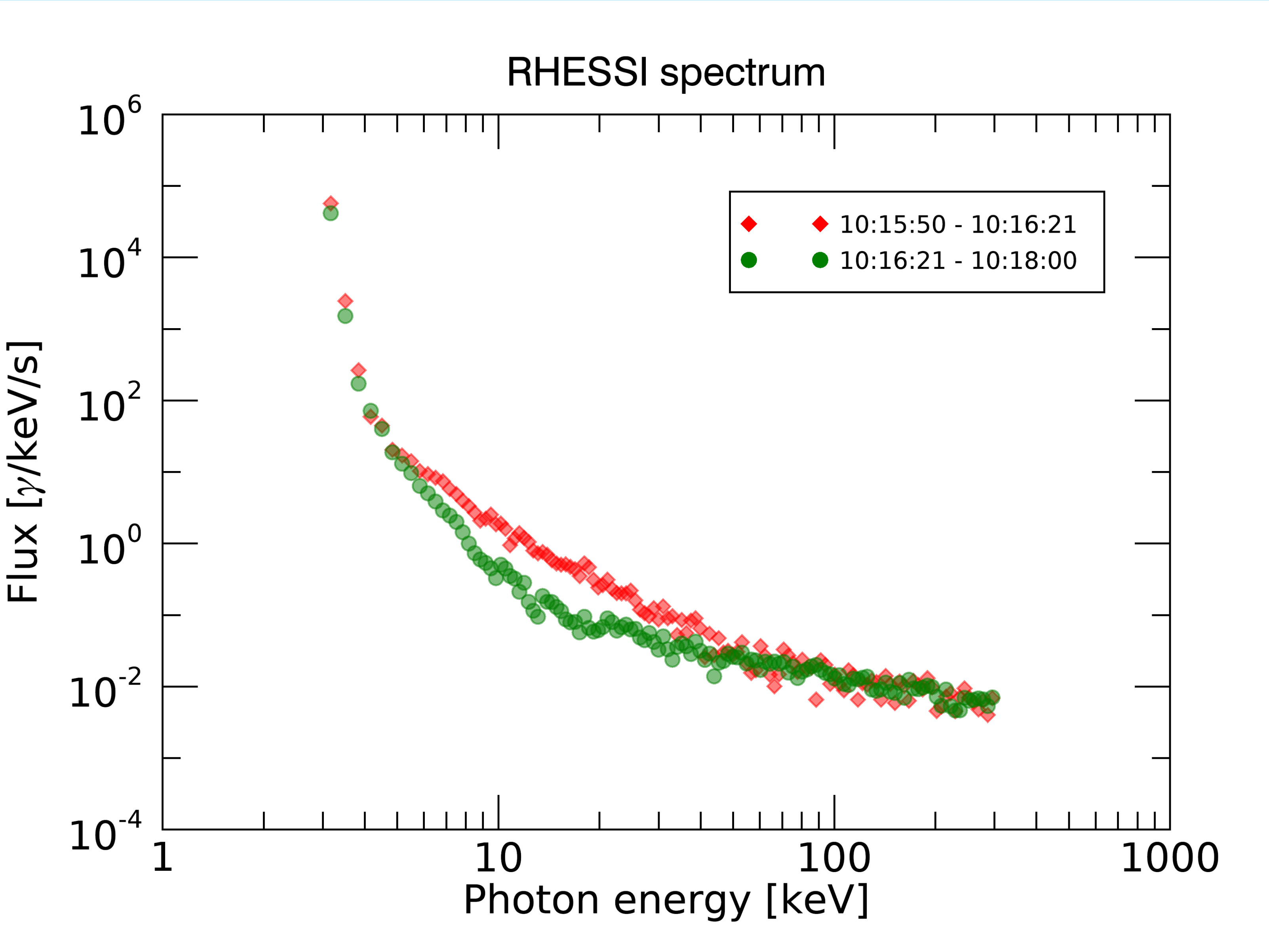
RHESSI spectrum
10:15:50 - 10:16:21
10:16:21 - 10:18:00
Flux [γ/keV/s]
10^6
10^4
10^2
10^0
10^-2
10^-4
1
10
100
1000
Photon energy [keV]

SDO/HMI

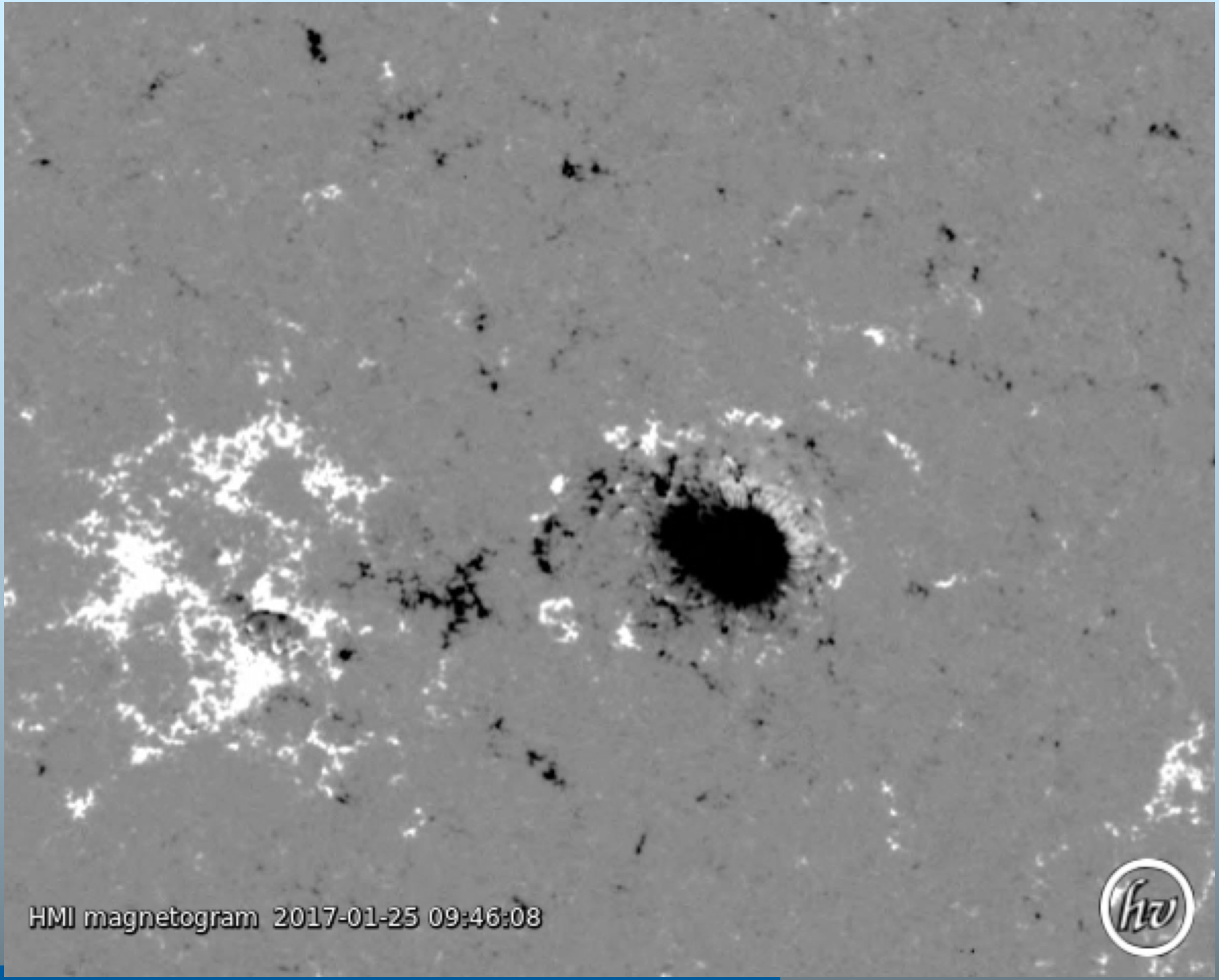

SDO/HMI

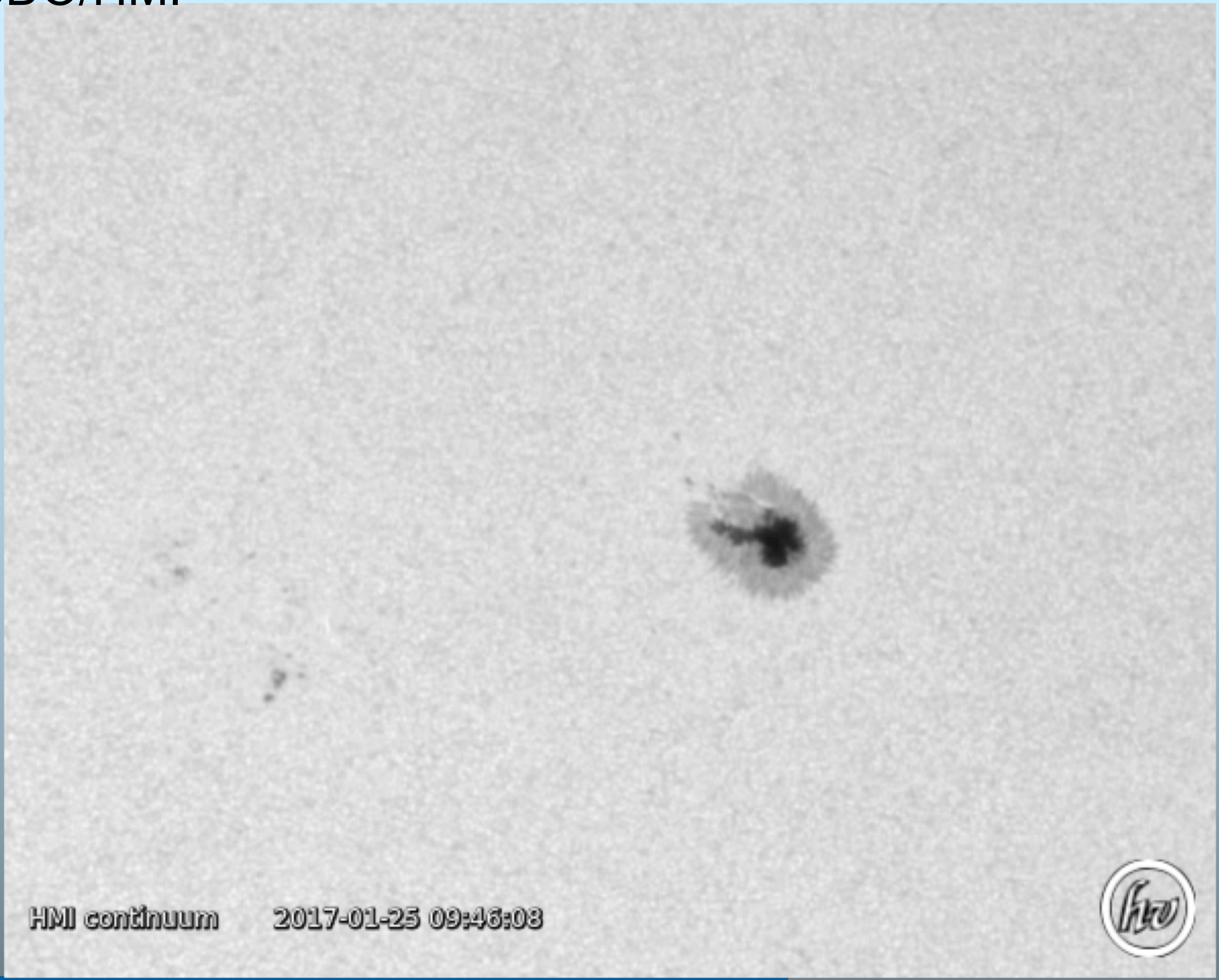

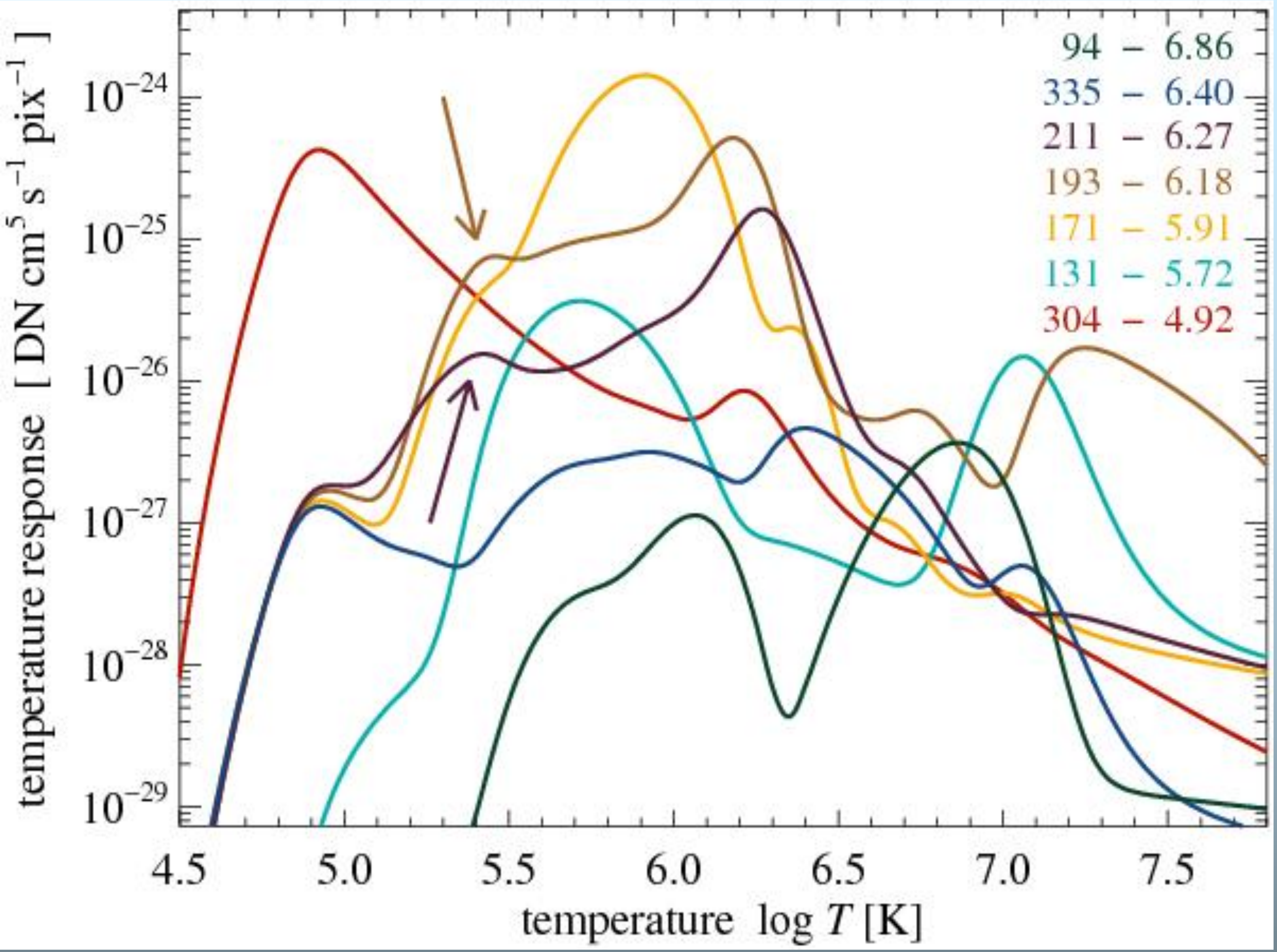
94 – 6.86
335 – 6.40
211 – 6.27
193 – 6.18
171 – 5.91
131 – 5.72
304 – 4.92
temperature response [DN cm^5 s^-1 s^-1 pix^-1]
10^-24
10^-25
10^-26
10^-27
10^-28
10^-29
4.5
5.0
5.5
6.0
6.5
7.0
7.5
temperature log T [K]

SDO/AIA 1700A

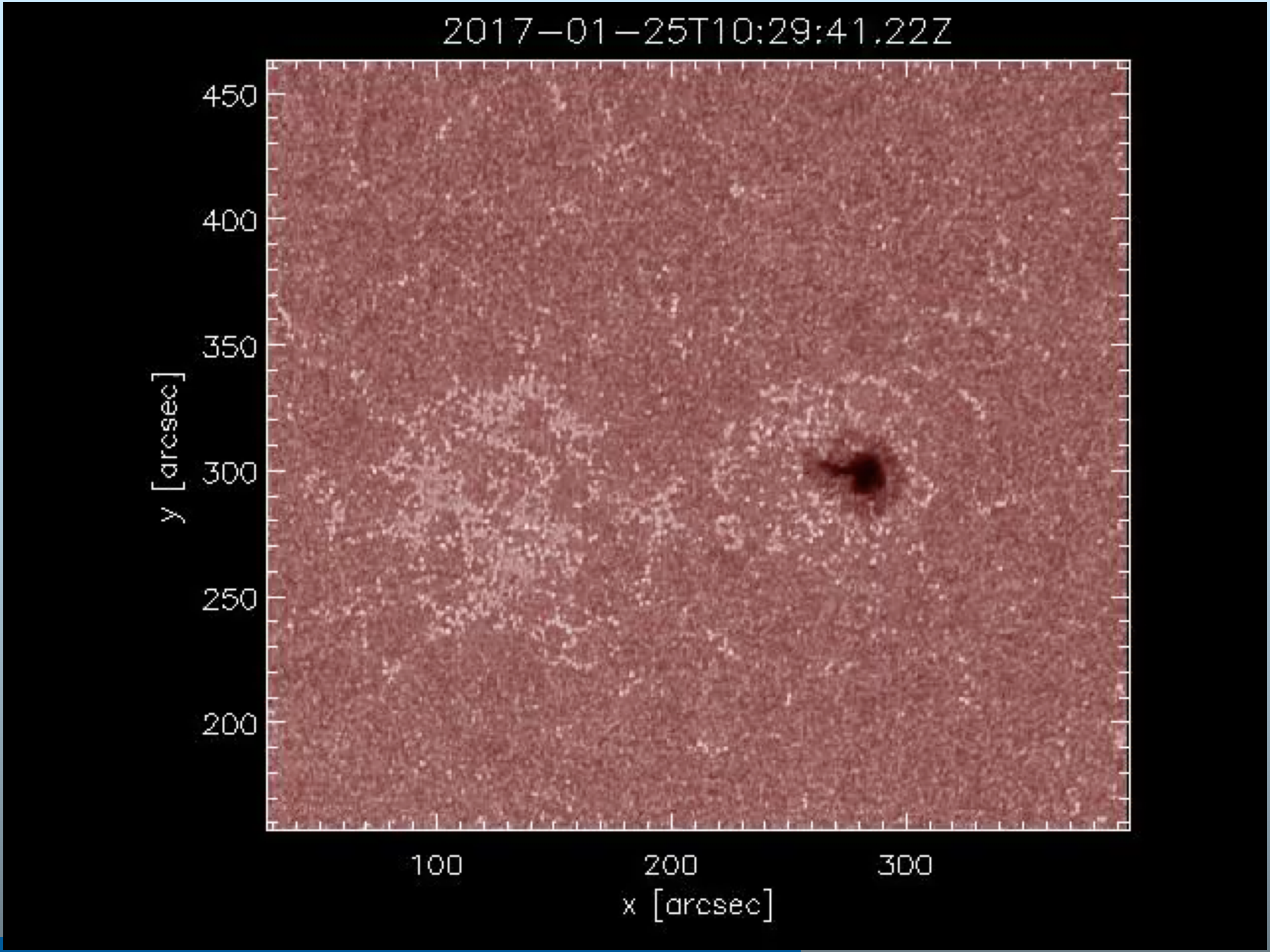

SDO/AIA 1600A

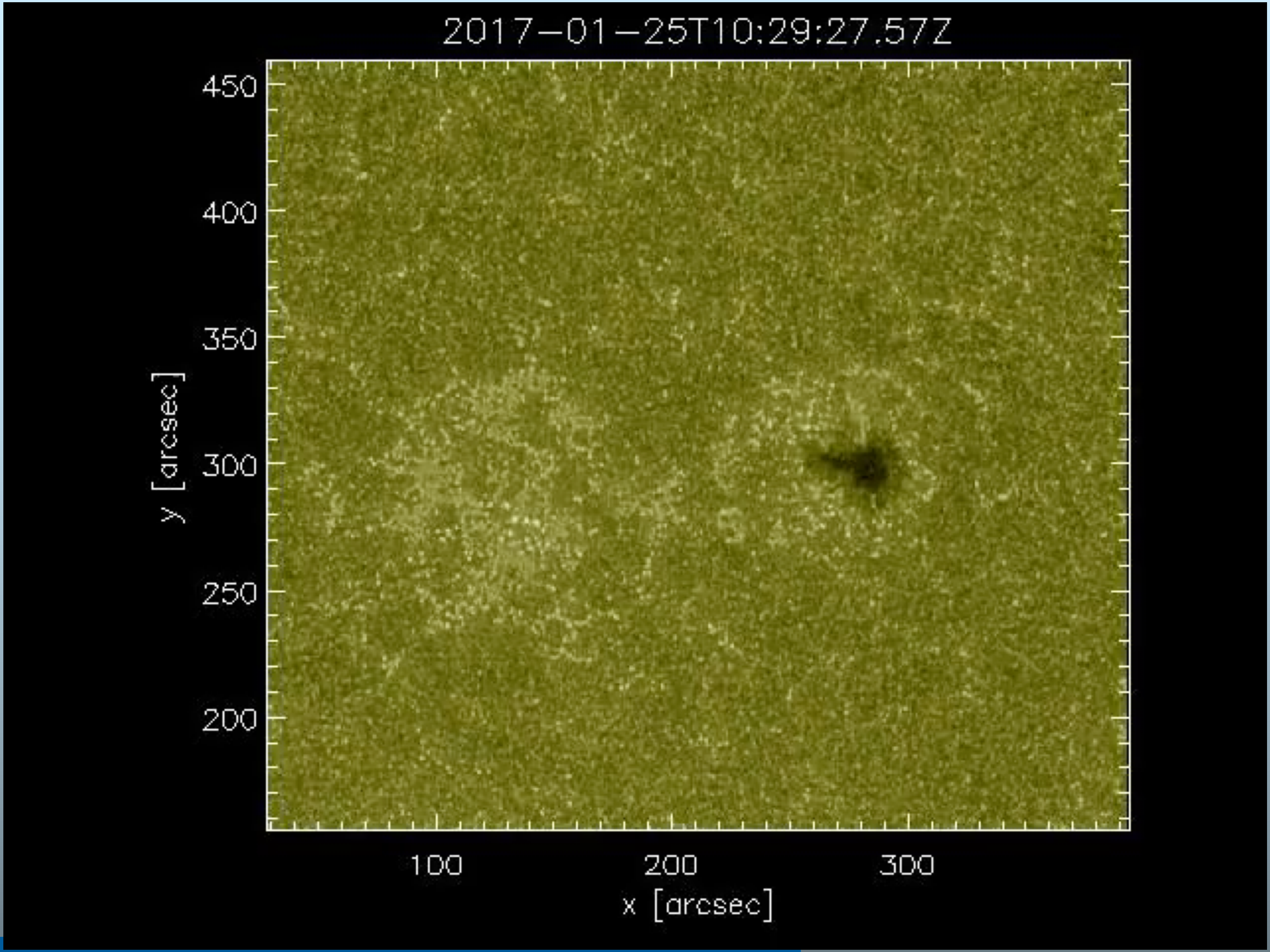

SDO/AIA 171A

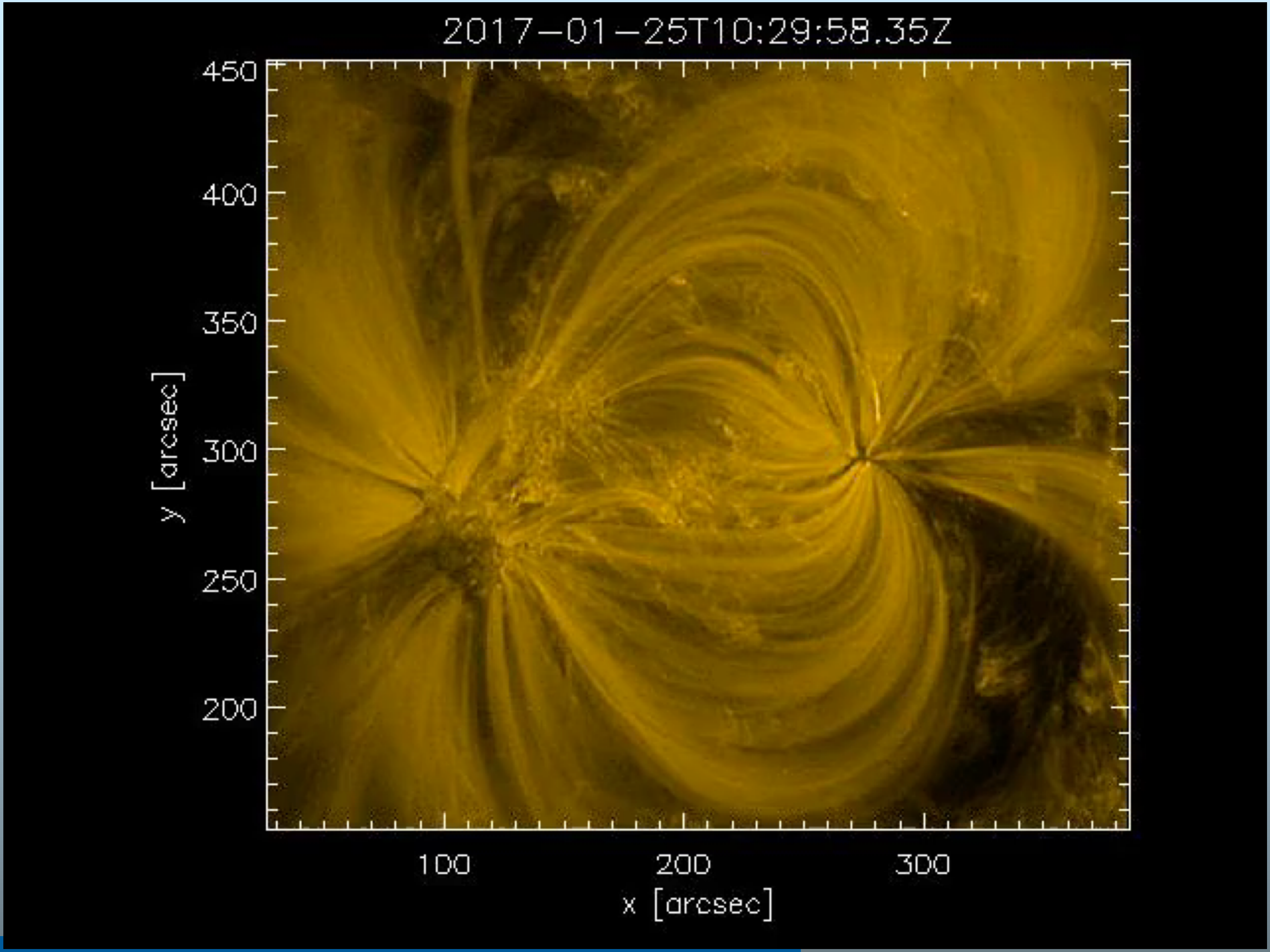
2017−01−25T10:29:58.35Z
450
400
350
300
250
200
y [arcsec]
100
200
300
x [arcsec]

SDO/AIA 193A

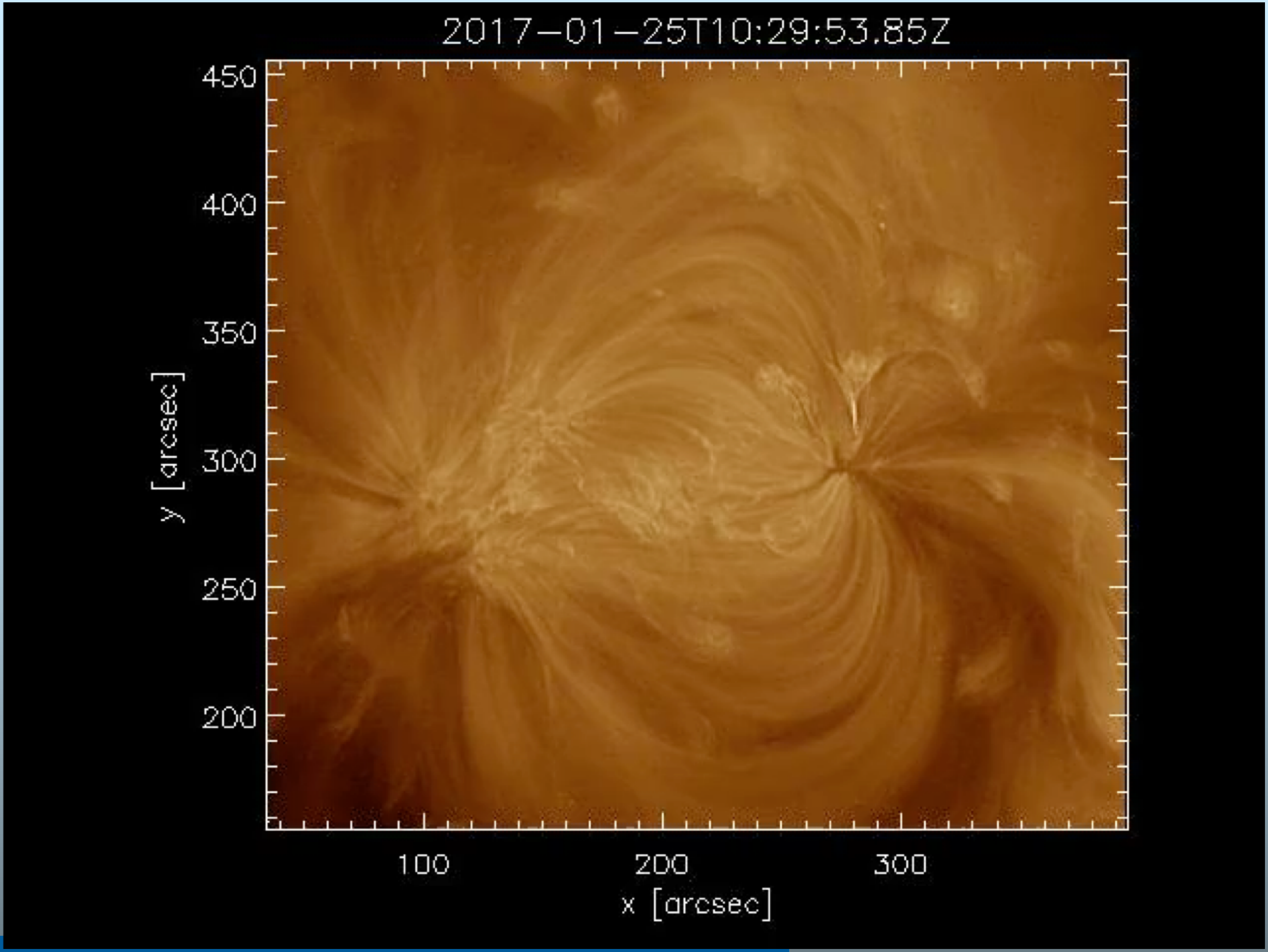

2017-01-25T10:29:53.85Z
450
400
350
300
250
200
y [arcsec]
100
200
300
x [arcsec]

SDO/AIA 131A

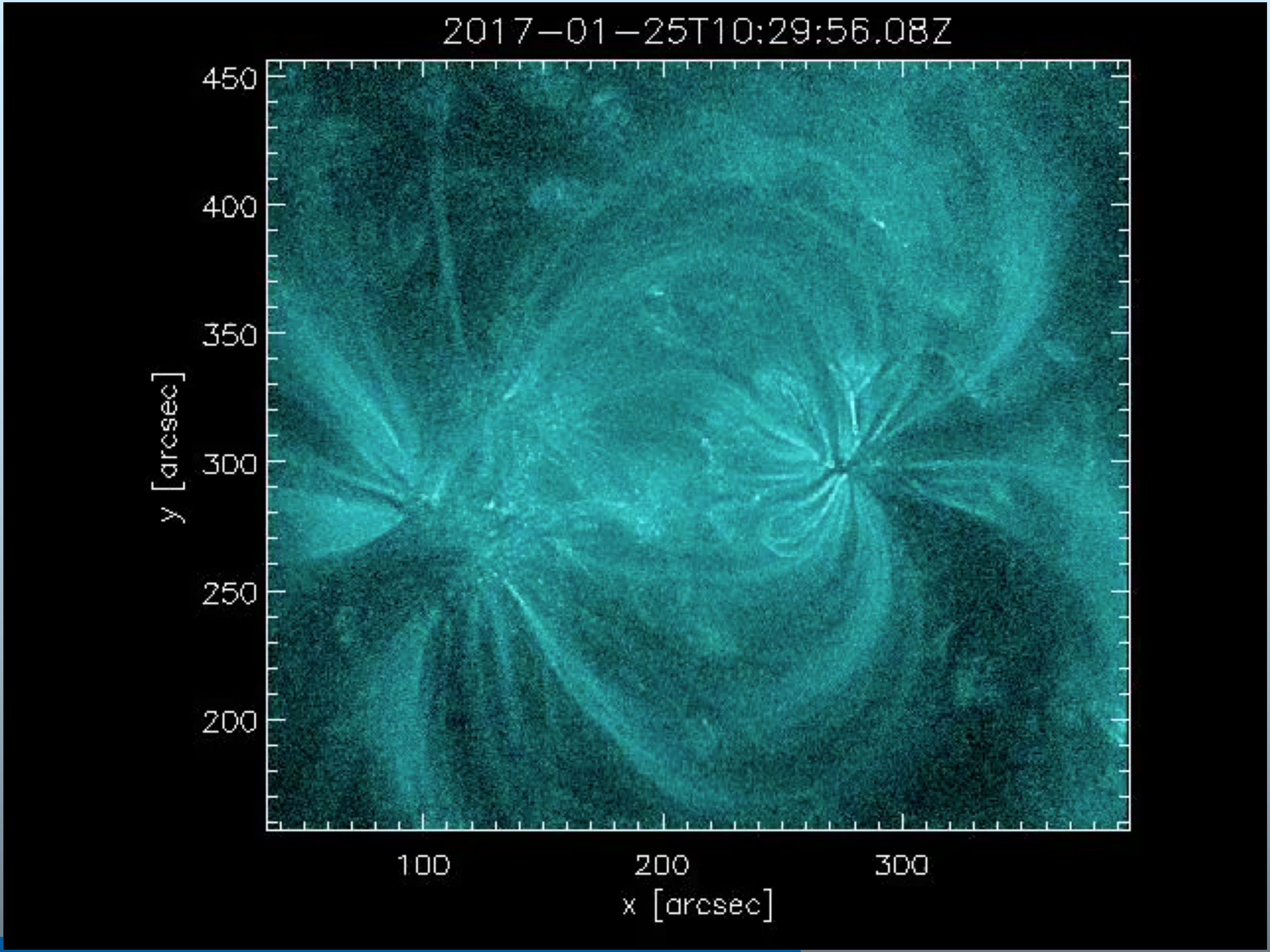
2017-01-25T10:29:56.08Z
450
400
350
300
250
200
y [arcsec]
100
200
300
x [arcsec]

SDO/AIA 94A

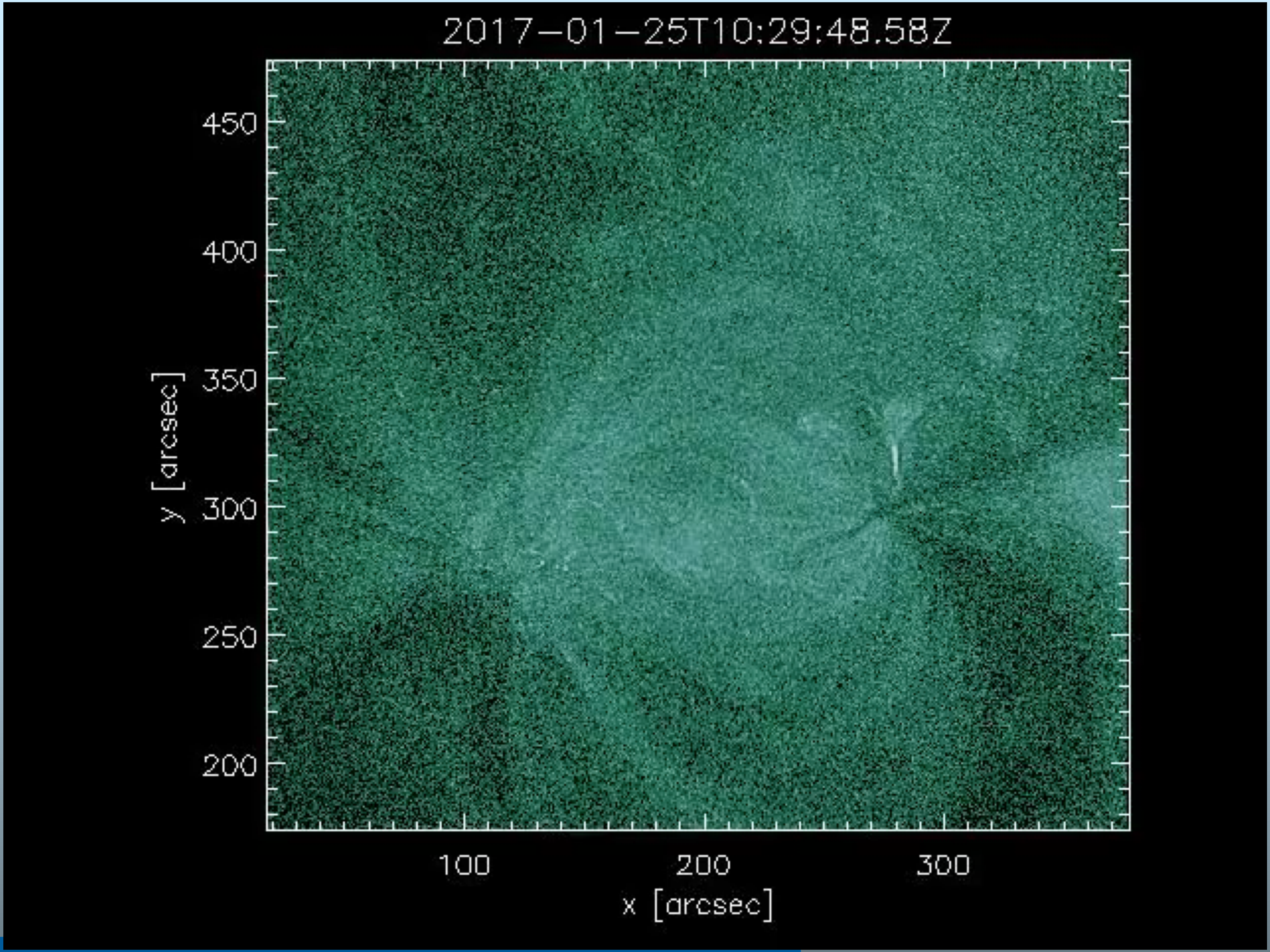
2017-01-25T10:29:48.58Z
450
400
350
300
250
200
y [arcsec]
100
200
300
x [arcsec]

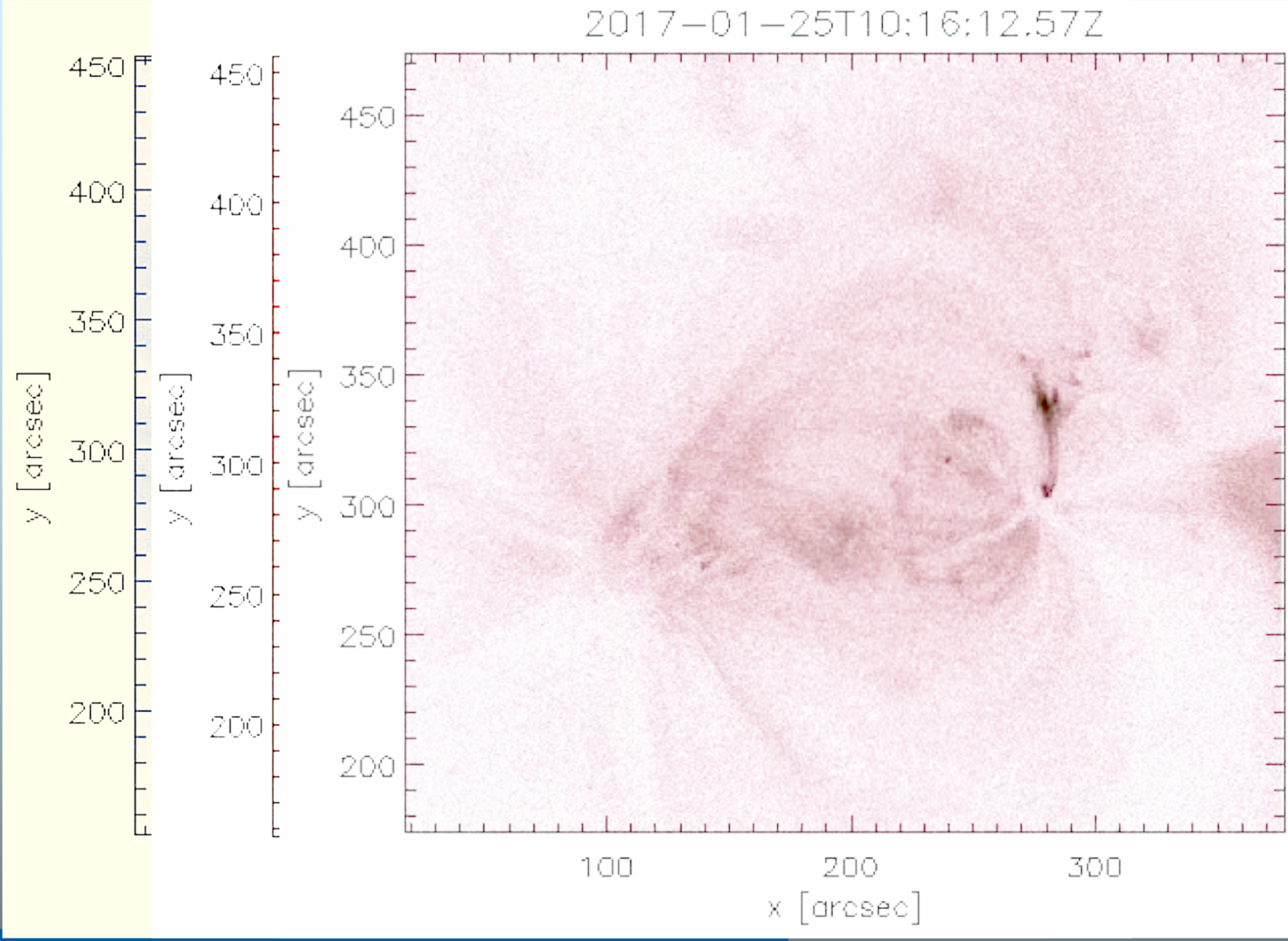
2017–01–25T10:16:12.57Z
450
400
350
300
250
200
y [arcsec]
100
200
300
x [arcsec]

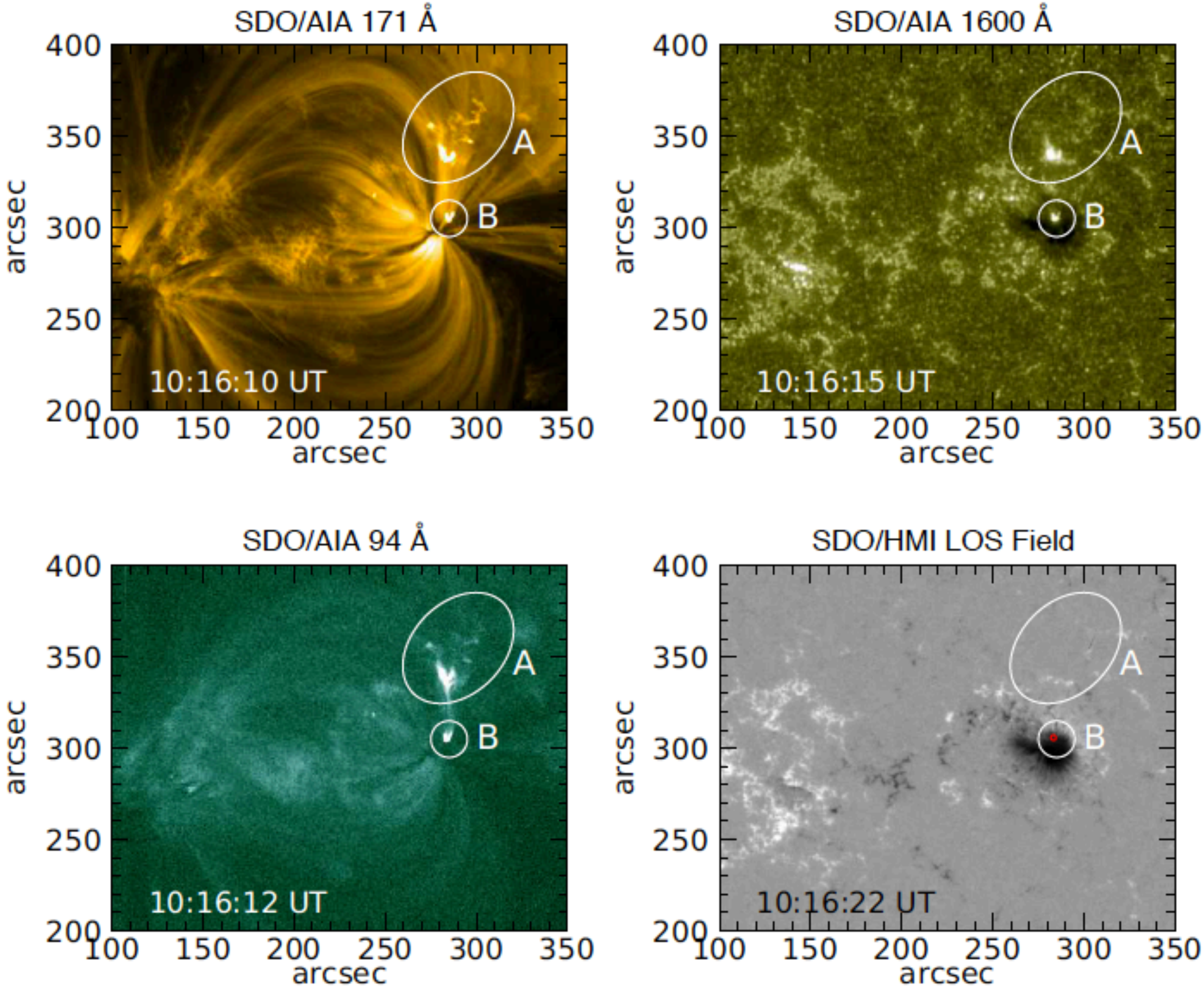
SDO/AIA 171 Å
10:16:10 UT
SDO/AIA 1600 Å
10:16:15 UT
SDO/AIA 94 Å
10:16:12 UT
SDO/HMI LOS Field
10:16:22 UT
A
B
arcsec
400
350
300
250
200
100
150
200
250
300
350

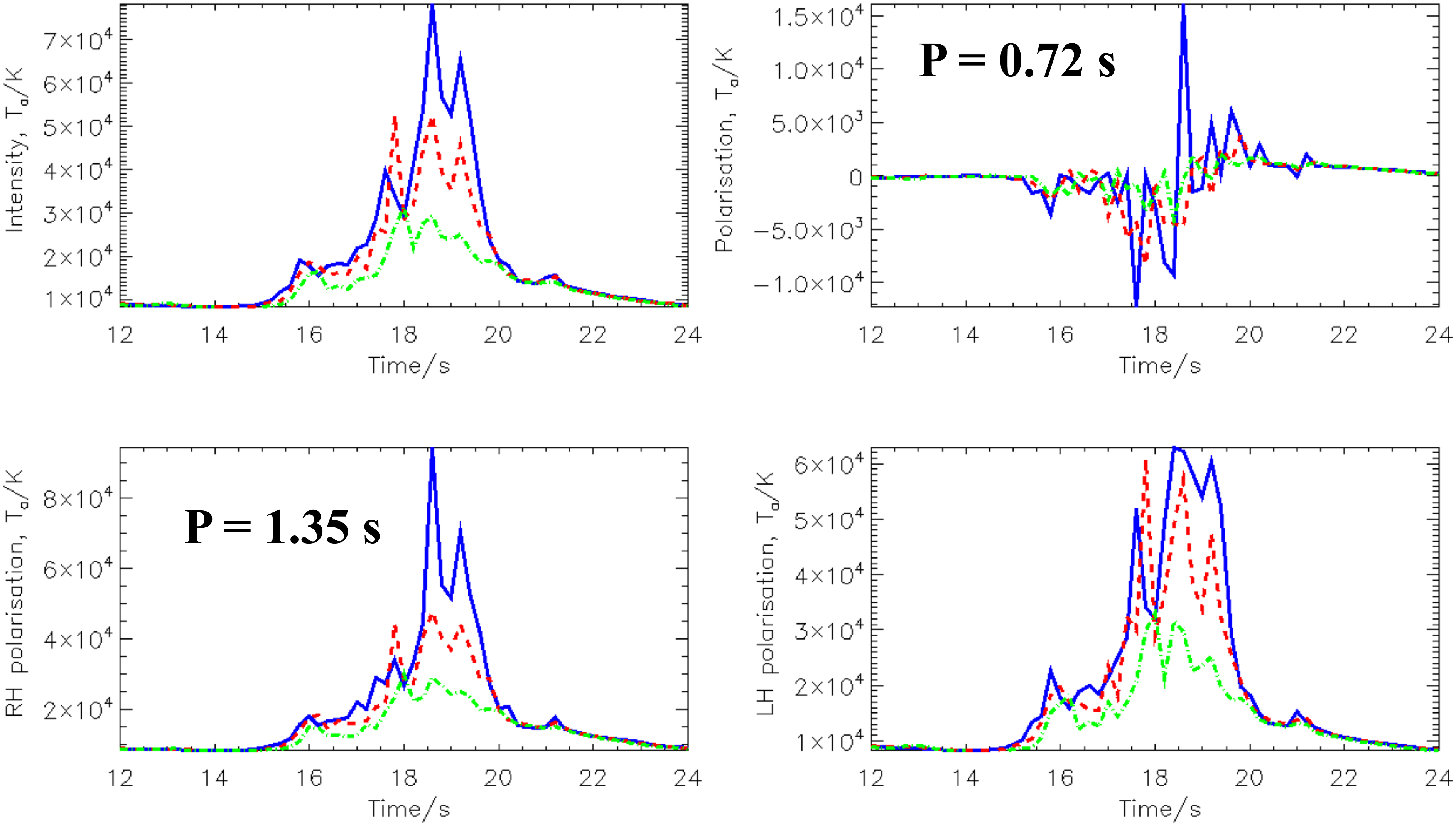

Blue - 3.090 GHz
Red - 3.281 GHz
Green - 3.468 GHz

If emission on f_{pe}
(plasma mechanism):
$n_e = 1.111 \times 10^{17} m^{-3}$
$n_e = 1.275 \times 10^{17} m^{-3}$
$n_e = 1.452 \times 10^{17} m^{-3}$
($f_{pe}[Hz] = 9x\ n_e^{1/2}[m^{-3}]$)

If emission on f_{ce}
(gyroresonant mechanism):
B_0 = 1071 G (1st), 357 G (3rd)
B_0 = 1147 G (1st), 383 G (3rd)
B_0 = 1225 G (1st), 408 G (3rd)
($f_{ce}[Hz] = 2.8x10^6\ B[G]$)

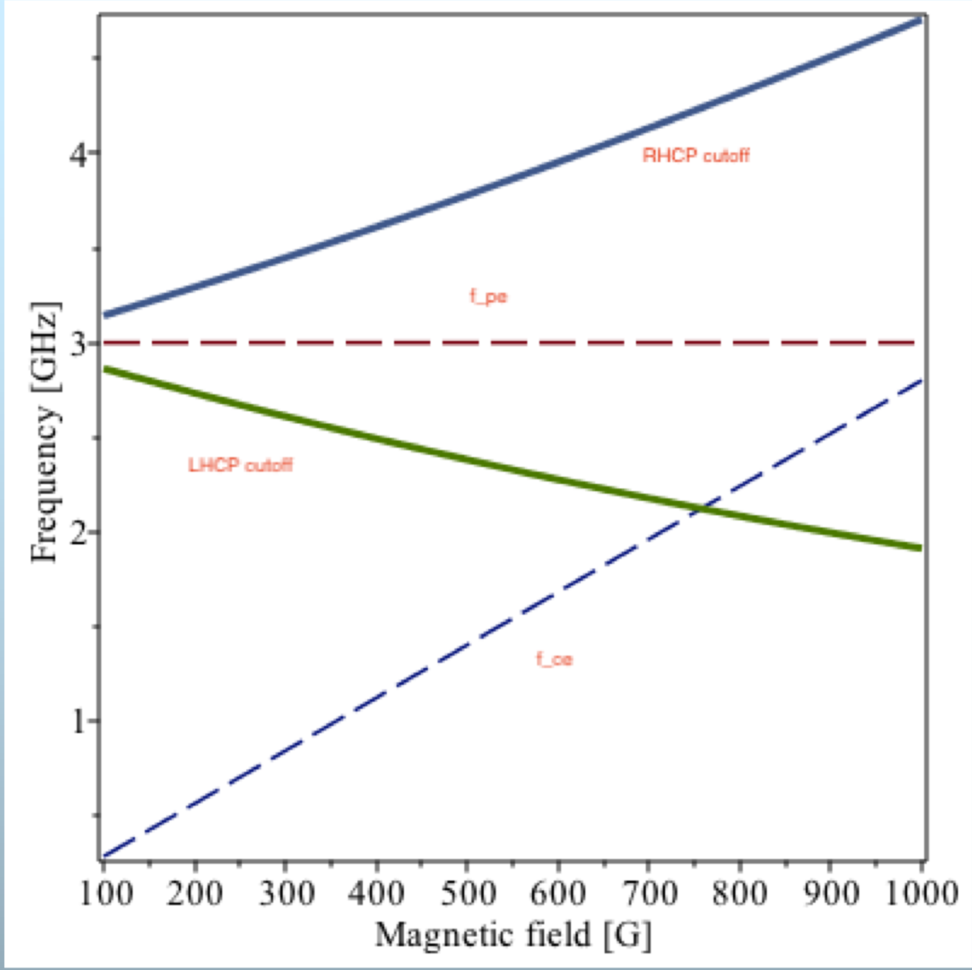

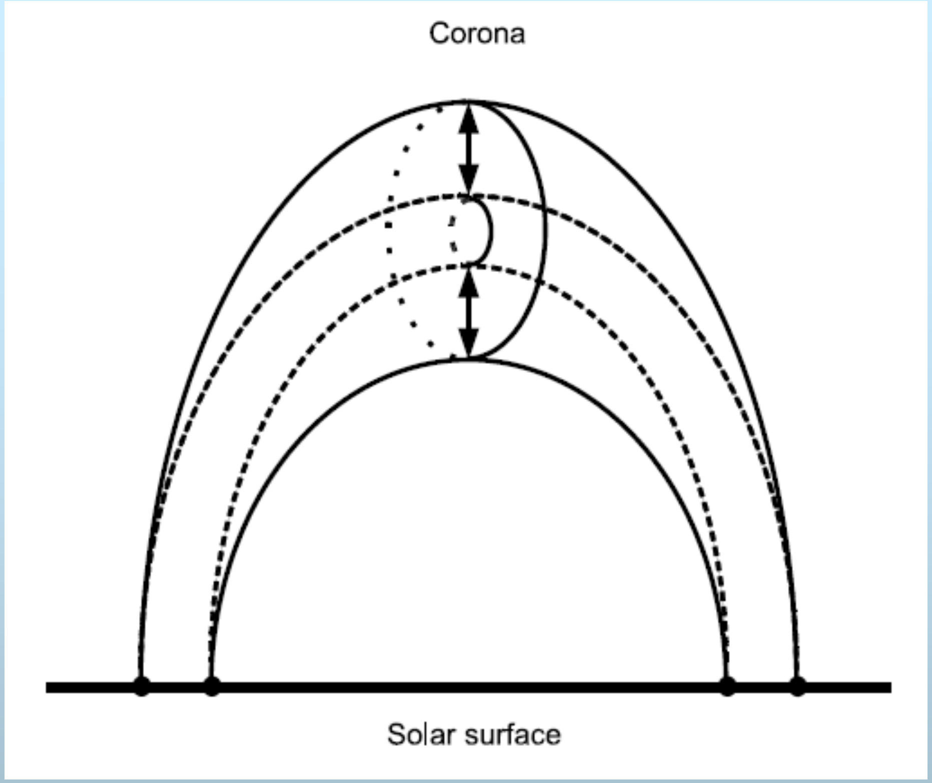

Sausage mode can **modulate the emission from footpoints** through the modulation of the mirror ratio of non-thermal electrons

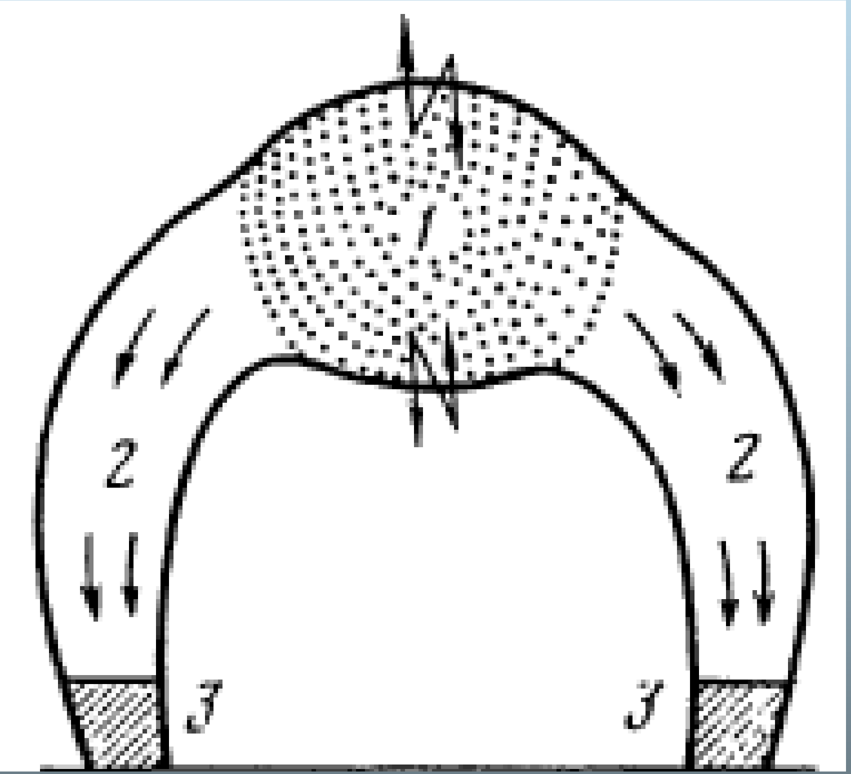

The Zaitsev-Stepanov mechanism

Zaitsev, V. V., & Stepanov, A. V. 1982, Soviet Ast., 26, 340

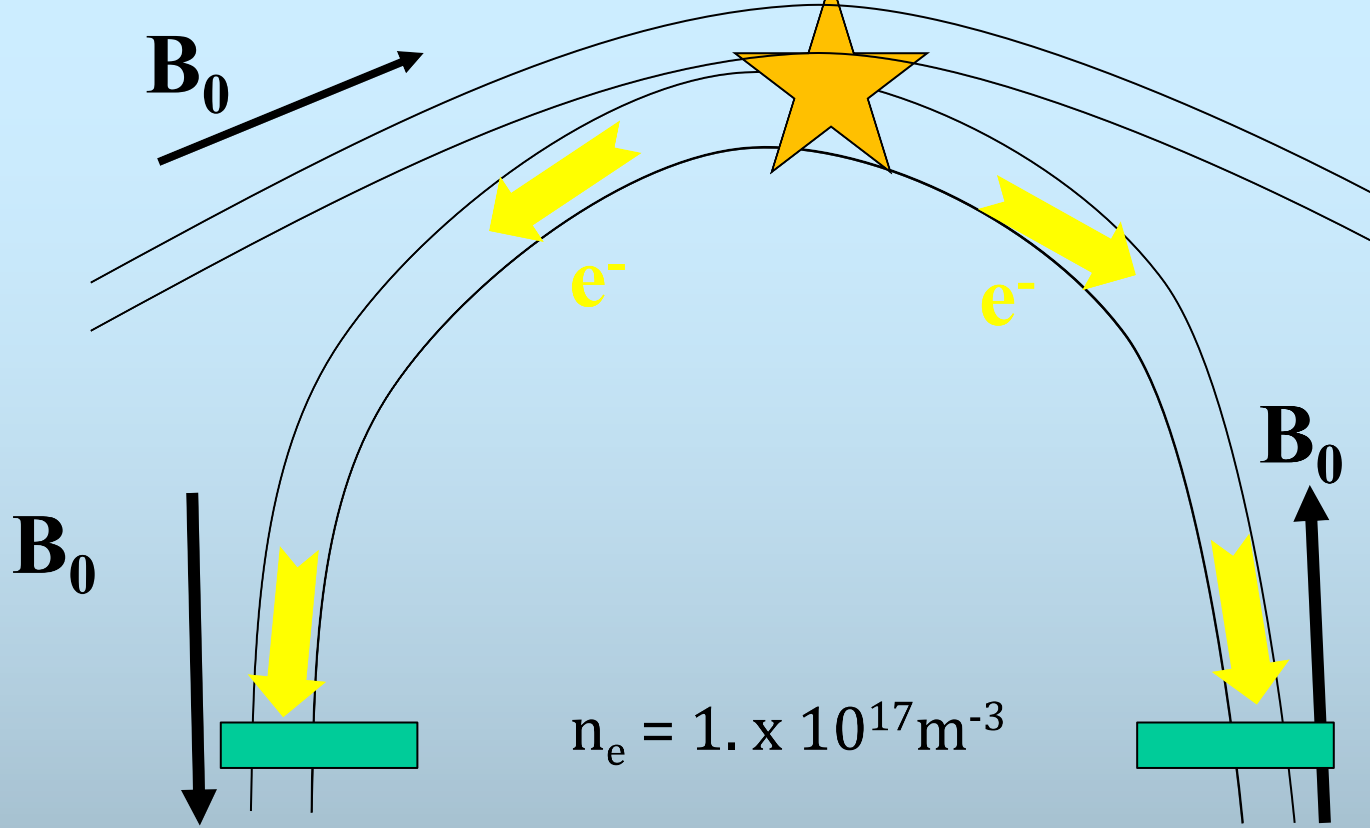

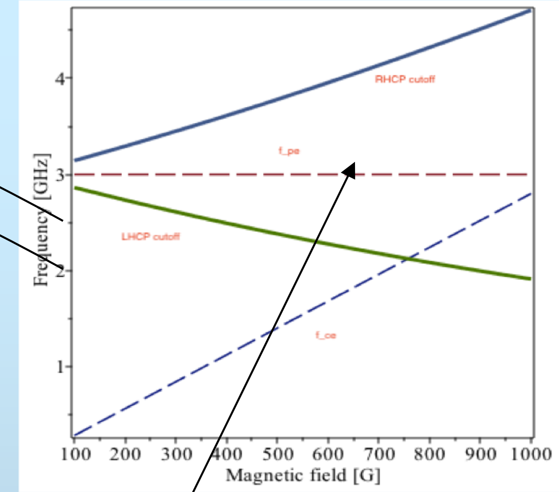

Only the LHCP wave goes upward

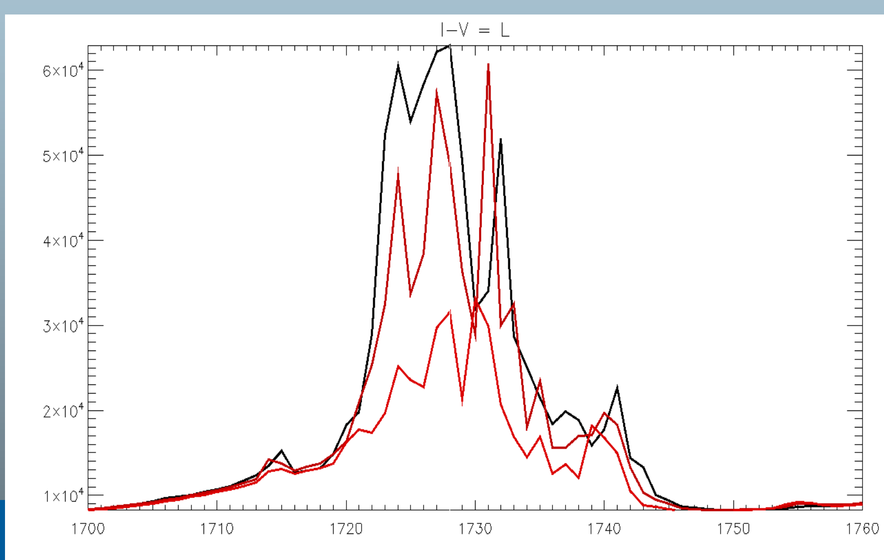

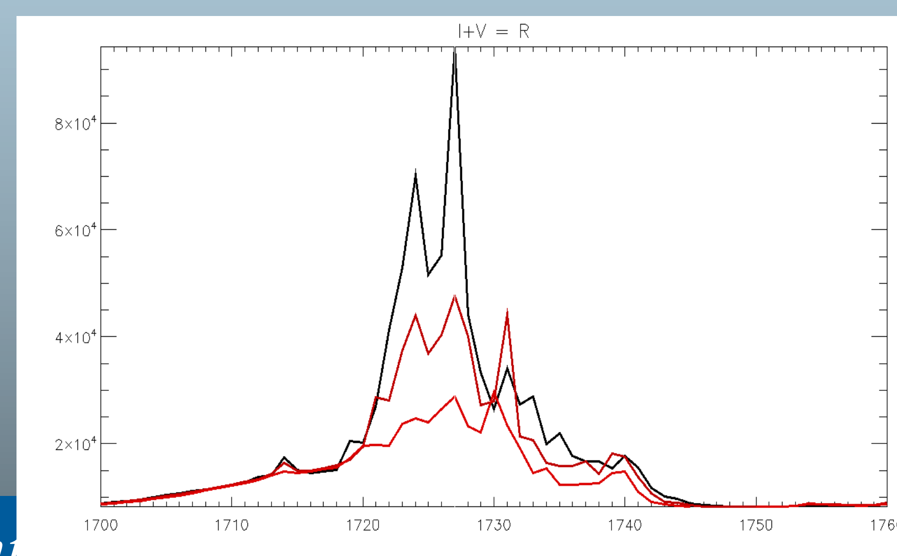

What is going on, and why?

- The event is associated with a microflare.
- There are non-thermal electrons.
- The intensity decreases with frequency very rapidly.
- LHCP and RHCP are seen of similar intensity and synchronous.

- The observed emission could be produced at f_{pe} by non-thermal electrons interacting with the TR ($n_e = 10^{17} m^{-3}$).
- LHCP and RHCP waves come from different footpoints, but from the same height ($n_e = 10^{17} m^{-3}$).
- The observed modulation is connected with a quasi-periodic process affecting the non-thermal electrons (sausage oscillation?, oscillation of the x-point?, …)

Sausage mode:

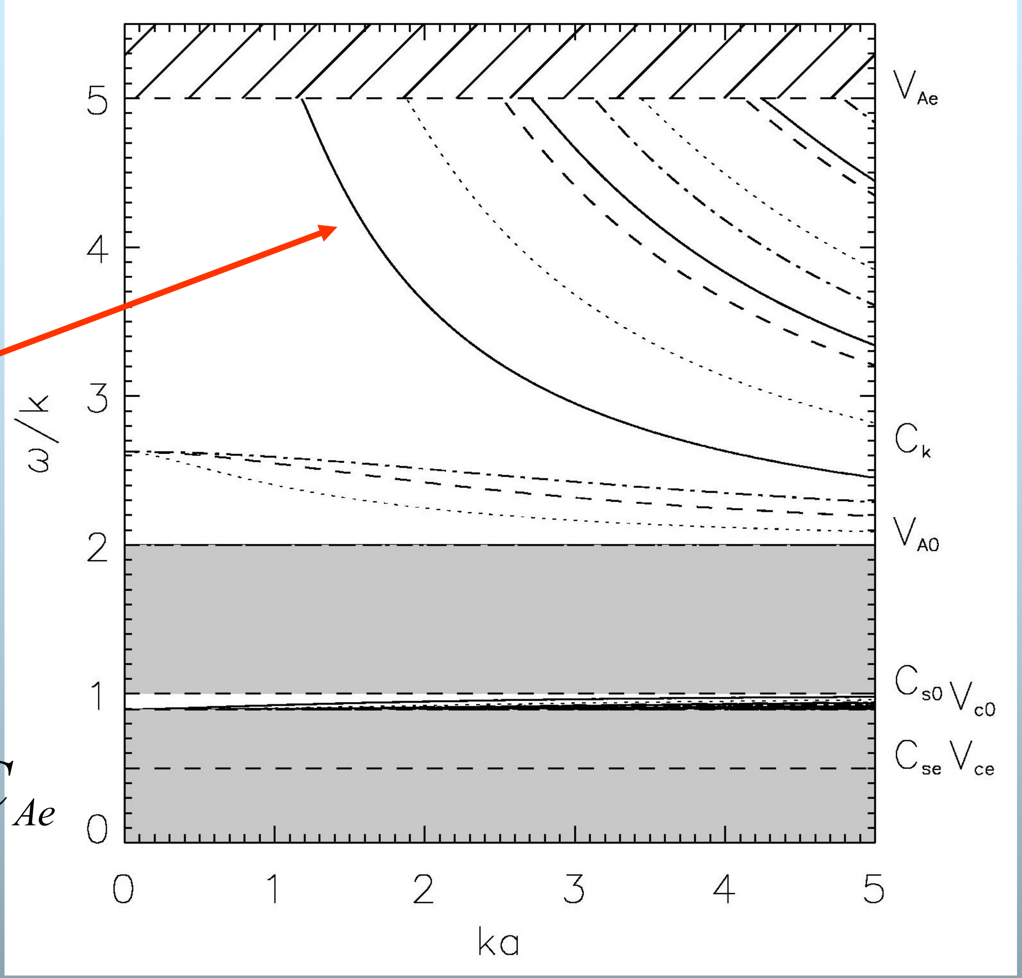

m=0 mode

In the **trapped** regime:

$$P_{GSM} = 2L / C_P, \quad C_{A0} < C_P < C_{Ae}$$

$$P < \frac{2\pi a}{j_0 C_{A0}} \approx \frac{2.62a}{C_{A0}}$$

In solar corona:

P = 1-60 s

Conclusions:

- Detection of QPP in microflares allows provides us with a useful (possibly, unique) information for revealing physical mechanisms operating in them.

- The event on 25 Jan 2017 shows an interesting irregular QPP in polarisation, with the characteristic time scale of about 0.7 s.

- Good evidence that the both the signals of the apparent LHCP and RHCP are actually caused by the superposition of two LHCP signals coming from the opposite legs of a magnetic flux tube.

- The characteristic time scales of the QPP are consistent with sausage oscillations of the flaring loop.

PHYSICAL REVIEW E **93**, 053205 (2016)

Nonlinear oscillations of coalescing magnetic flux ropes

Dmitrii Y. Kolotkov,* Valery M. Nakariakov,† and George Rowlands
Centre for Fusion, Space and Astrophysics, Department of Physics, University of Warwick, CV4 7AL, United Kingdom
(Received 11 February 2016; published 19 May 2016)

An analytical model of highly nonlinear oscillati
ropes, based upon two-fluid hydrodynamics, is devel